Elucidation of the Role of Peroxisome Homeostasis in *Drosophila* Embryogenesis

A Thesis

submitted to

Indian Institute of Science Education and Research Pune in partial fulfilment of the requirements for the BS-MS Dual Degree Programme

by

Shweta Garg

(20191113)

Indian Institute of Science Education and Research Pune

Dr. Homi Bhabha Road,

Pashan, Pune 411008, INDIA.

Date: March, 2024

Under the guidance of

Supervisor: Dr. Richa Rikhy,

Department of Biology, IISER Pune

Certificate

This is to certify that this dissertation entitled ***"Elucidation of the Role of Peroxisome Homeostasis in Drosophila Embryogenesis"*** towards the partial fulfilment of the BS-MS dual degree programme at the Indian Institute of Science Education and Research, Pune represents study/work carried out by **Shweta Garg** at Indian Institute of Science Education and Research, Pune under the supervision of **Dr. Richa Rikhy, Professor, Division of Biology, IISER Pune** during the academic year 2023-24.

Dr. Richa Rikhy

Professor

Division of Biology, IISER Pune

Committee -

Prof. Richa Rikhy (Supervisor)

Prof. Girish Ratnaparkhi (TAC member)

This thesis is dedicated to my supervisor, Dr. Richa Rikhy and to my family and friends.

Declaration

I hereby declare that the matter embodied in the report entitled ***"Elucidation of the Role of Peroxisome Homeostasis in Drosophila Embryogenesis"*** are the results of the work carried out by me at the Department of Biology, Indian Institute of Science Education and Research, Pune, under the supervision of **Dr. Richa Rikhy** and the same has not been submitted elsewhere for any other degree.

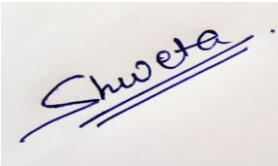

Shweta Garg

20191113

Table of Contents

List of Tables

List of Figures

Chapter 1

Abstract

Peroxisomes are subcellular organelles that play a crucial role in metabolism, reactive oxygen species (ROS) detoxification, and cellular signaling. Embryogenesis requires the coordinated function of organelles and cytoskeleton to give rise to epithelial-like cells. Previous studies from the lab have highlighted the significance of appropriate morphology, distribution and function of mitochondria in the morphogenetic processes involved in cell formation during *Drosophila* embryogenesis. However, the role of peroxisomes, an organelle that interacts with mitochondria, in regulating the different steps of cell formation and remodeling remains to be elucidated. Our results show that peroxisomes accumulate apically similar to mitochondria with the progression of cellularization. In embryos depleted for Drp1 (dynamin-related protein 1), which is involved in mitochondrial and peroxisome fission in various systems, peroxisomes appear to be enlarged, predominantly showing a fused state and reduced number, suggesting a role for Drp1 in peroxisomal fission during *Drosophila* cellularization. Further, to shed light on the peroxisome formation in embryonic development, we employed RNAi to knock down various PEX proteins known to be involved in peroxisome biogenesis. Our results show the absence or reduction in the number of peroxisomes upon the knockdown of PEX13, PEX16, PEX19 and PEX3, indicating their role in peroxisome biogenesis in embryogenesis. We further tested the role of ROS in regulating the numbers of peroxisomes. Depletion of mitochondrially targeted SOD2 led to an increase in the numbers of peroxisomes and the suppression of the defects in peroxisomes number in $Drp1^{SG}$; $sod2^{i}$ mutant. This indicates the peroxisome numbers are likely to respond to increased oxidative stress, aiding ROS removal.

Acknowledgments

I am profoundly grateful to my mentor, supervisor, and guide, Dr. Richa Rikhy, for entrusting me with the invaluable opportunity to contribute to this project. Dr. Rikhy's unwavering support, guidance, and encouragement have been indispensable throughout every stage of this project. Her innovative ideas and unwavering commitment to exploring new methodologies have propelled our research forward. Dr. Rikhy's expertise and willingness to assist me in navigating challenges, whether they be experimental or technical in nature, have been instrumental. Without Dr. Rikhy's steadfast support and visionary leadership, this project would not have reached its fruition. I am deeply grateful for her mentorship and the trust she placed in me to execute her ideas.

Furthermore, I extend my sincerest appreciation to all my esteemed lab members—Bhavin, Somya, Debasmita, Rahul, Sanjana, Harsh, Aparna, Anirban, Shashwat, Bhavesh, and Atharva. Their collective support, camaraderie, and insights enriched the project immensely. I am indebted to each of them for their contributions and unwavering encouragement.

Nandeesh, who worked alongside me on this project, deserves special acknowledgment. His dedication and collaborative spirit were invaluable assets throughout our journey.

I also wish to express my gratitude to the individuals from other labs who generously shared their expertise and offered assistance whenever needed. Their willingness to lend a helping hand significantly contributed to the success of this project.

Lastly, I am profoundly thankful to my friends and family members for their unwavering support and encouragement. Their belief in my abilities provided the mental strength I needed to persevere and overcome obstacles throughout this journey.

Chapter 1 Introduction

1.1 Peroxisomes: Essential Players in Cellular Metabolism

In the eukaryotic cell there is an intricate network of organelles with its unique functions which are essential for coordination of complex biological processes. Among these, peroxisomes, have emerged as essential players in cellular metabolism, discovered as microbodies in 1954 by Rhodin, were previously believed to be just a waste disposal system or "fossil organelles" (Rhodin J 1954). But de Duve and Baudhuin's analysis in 1966 showed them to be active organelles containing oxidases such as catalase, which breaks down H2O2 (De Duve et al. 1966). As a result, these structures were renamed peroxisomes.

Peroxisomes are multifunctional organelles found in both prokaryotic and eukaryotic organisms, serving multiple functions. Unlike mitochondria and chloroplasts, they are encased within a single membrane and exhibit remarkable flexibility in morphology and metabolism. Their enzymatic composition and structure differ widely between organisms and cell types, indicating their ability to adapt to various environments. Peroxisomes come in varied sizes (0.1–1.5 µM) and shapes (usually round but can also be elongated or form a network) and their abundance varies depending on cell type and surroundings (Yamamoto et al. 1987). Mammals, for instance, have peroxisomes in the liver with the highest concentration, constituting approximately 2% of total protein content (Walker et al. 2018).

Functionally, peroxisomes play a role in numerous metabolic processes. These organelles play a crucial role in the breakdown and synthesis of lipids, a process known as lipid metabolism. Specifically, peroxisomes are responsible for the oxidation of very long-chain fatty acids (containing 22 or more carbon atoms) and branched-chain fatty acids, as well as the breakdown of purine molecules (Poirier et al. 2006) as shown in Fig.1. According to Fujiki et al. (2020), peroxisomes are involved in the biosynthesis of certain specialized fatty acids, including plasmalogens, and ether-lipids which are essential for various biological functions within the organism. Additionally, they control

levels of many reactive oxygen species. Peroxisomes have different functions depending on the organism. For instance, in plants, they play a key role in the metabolic pathway essential for the conversion of lipids into carbohydrates (glyoxylate cycle), necessary for seed germination and seedling growth**.** (Hayashi et al. 2000). They may also participate in cellular signaling pathways, which are still being studied. Despite some similarities to mitochondria in function, peroxisomes have a unique structure with a single membrane enclosing a concentrated enzyme matrix.

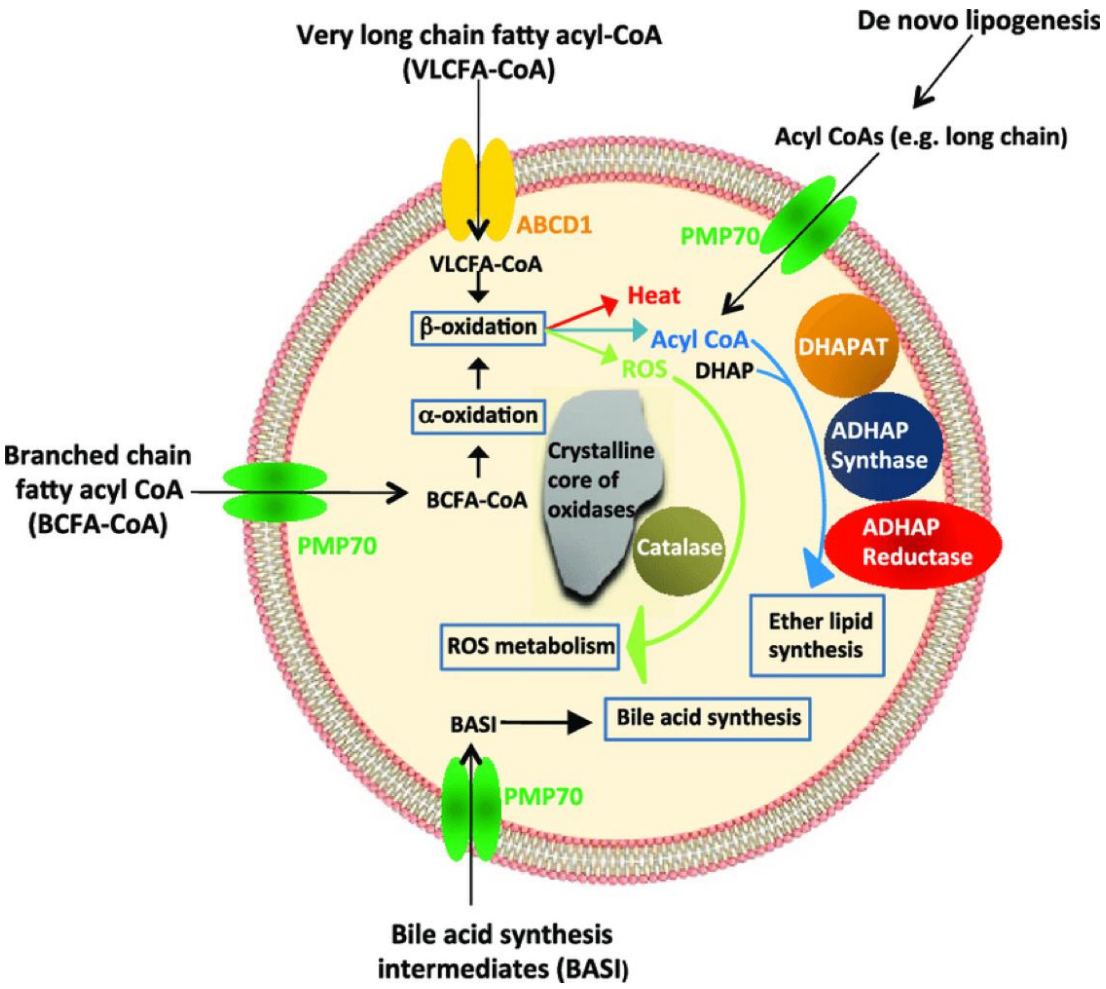

Figure 1 - Structure and Functions of Peroxisomes - Peroxisomes are intracellular organelles that are encased by the single-membrane and central to various metabolic processes within mammalian cells. Key functions include the breakdown of fatty acids containing an extensive number of carbon atoms through β-oxidation, converting fatty acids with branched structures through α-oxidation, producing bile acids and ether-linked phospholipids, and the elimination of ROS molecules (Lodhi et al. 2014).

Peroxisomes are essential for maintaining cell structure, important in plants and fungi. In yeast, they are essential for β-oxidation, whereas in mammals, this process mainly happens in mitochondria (Knoblach et al. 2018). Despite this, peroxisomes can step in and process different fatty acids if mitochondrial function is impaired. They are closely connected with other cell components like the endoplasmic reticulum (ER), mitochondria, lipid droplets, and lysosomes. Notably, mutations in genes responsible for peroxisome assembly or function can result in a spectrum of human diseases termed peroxisome biogenesis disorders. These disorders can range from mild to life-threatening, highlighting the critical role of peroxisomes in maintaining cellular health (Steinberg et al. 2006).

In conclusion, peroxisomes are versatile and indispensable organelles in our cells, which are known to play an important functions in metabolism, ROS regulation, and potentially even signaling. Their versatility and complex role in cellular processes make them intriguing subjects for future study. Unraveling their roles and how they contribute to disease development may pave the way for the creation of innovative treatment strategies in the future.

1.2 Insights into Peroxisome Biogenesis: Pathways and Mechanisms

Unlike mitochondria, nuclei, and chloroplast, peroxisomes lack DNA. The nucleus contains the genetic information required for all peroxisome proteins, which are produced in the cytosol and later moved to the peroxisomes by a complex protein transport system. The exact mechanisms by which peroxisomes form and divide are still being unraveled. Current models suggest that they can either grow and divide from existing ones or be assembled from smaller building blocks.
Four main pathways have been reported in the literature for peroxisome formation (Deori et al. 2018) -

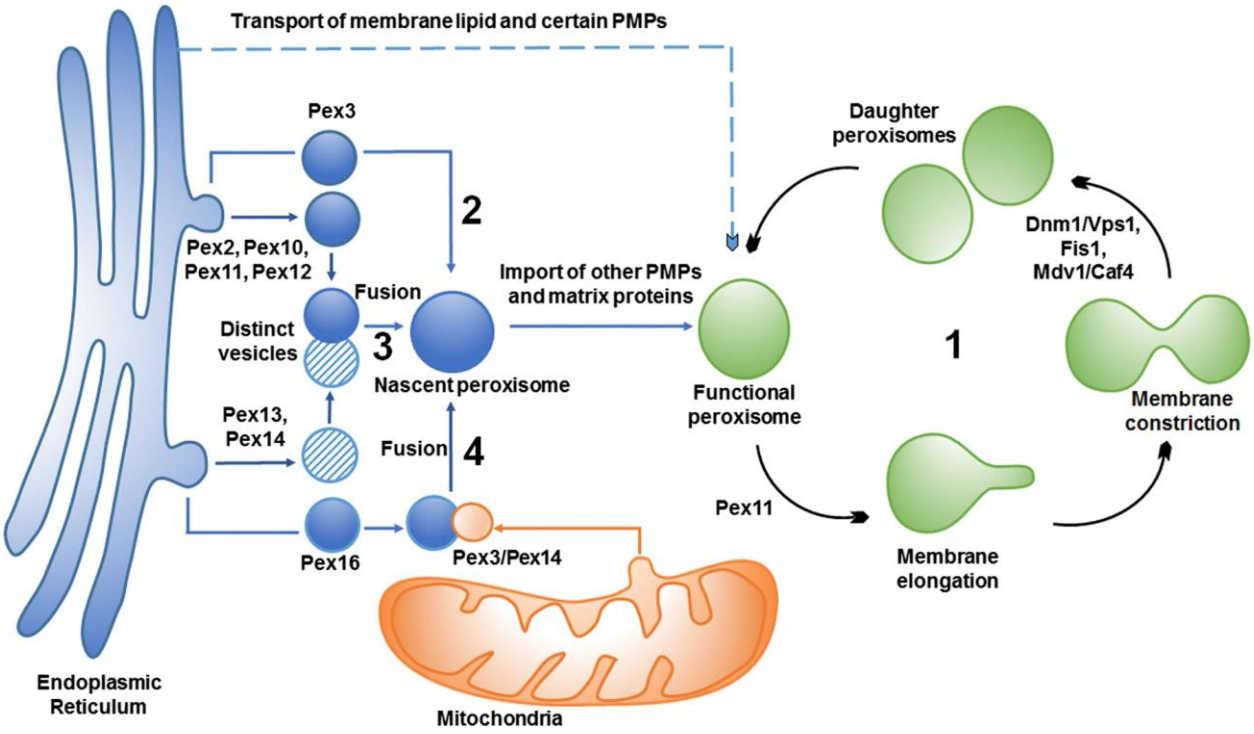

Figure 2 - The diverse mechanisms of peroxisomes formation (Deori et al. 2018).

1. **Peroxisome Multiplication through Division:** The process shown in Figure 2 includes the splitting of existing peroxisomes, a pathway observed in diverse various model organisms (Koch et al., 2003). Pex11, Dnm1, and Fis1 are involved in the splitting of the peroxisomes as part of the elongation and fission machinery (Opaliński et al., 2011). Initially, Pex11 promotes membrane elongation, followed by recruitment of Dnm1 by Fis1 for final scission. Adapter proteins like Mdv1 and Caf4 are necessary in yeast (Nagotu et al., 2008). Daughter peroxisomes develop into active organelles by bringing in matrix and membrane proteins, with the ER potentially aiding in lipid transport and certain peroxisomal membrane proteins (PMPs) (Raychaudhuri and Prinz, 2008).

2. **ER-Mediated Restoration of Functional Peroxisomes:** Loss of certain PMPs, such as PEX3, results in dysfunctional peroxisomes, which can be restored by reintroducing these PMPs (Hoepfner et al., 2005). In the event of non-functional peroxisomes, peroxisomal membrane proteins (PMPs) traverse the endoplasmic

reticulum (ER) and leave as pre-peroxisomal vesicles (ppVs) as shown in Fig. 2. These ppVs mature into functional peroxisomes by importing newly synthesized PMPs and other proteins found in the matrix before entering growth and division pathways.

3. **Formation of Peroxisomes from ER-Derived Vesicles**: Some studies indicate that the PMPs primarily traffic via ER, emerging as separate vesicles later forming nascent peroxisomes (van der Zand et al., 2012). Subsequently, the fusion of these vesicles occurs, allowing the incorporation of matrix proteins and additional PMPs, thereby establishing functional, metabolically active peroxisomes (Agrawal et al., 2016) as shown in Fig. 2.

4. **Mitochondria-Mediated Peroxisome Formation in Mammalian Cells**: When peroxisomes are missing, some PMPs end up in mitochondria and cause a fusion between vesicles containing PEX3/PEX14 that emanate from mitochondria and vesicles harboring PEX16 that originate from the endoplasmic reticulum, resulting in the formation of precursor vesicles for peroxisomes (Sugiura et al., 2017). The additional introduction of PMPs and matrix proteins converts these peroxisome precursor vesicles into operational peroxisomes (refer to Fig. 2).

1.2.1 Shared Fission Machinery Between Peroxisomes and Mitochondria

Peroxisomes, like mitochondria, modulate their morphology, abundance, and function to adapt to changing cellular demands or environmental cues. Their size and appearance can vary among tissues, indicating their versatility in responding to cellular needs. Remarkably, the control of peroxisome membrane dynamics is closely linked to the dynamics of mitochondria, jointly utilizing shared mechanisms for the processes of

division and formation of new organelles.

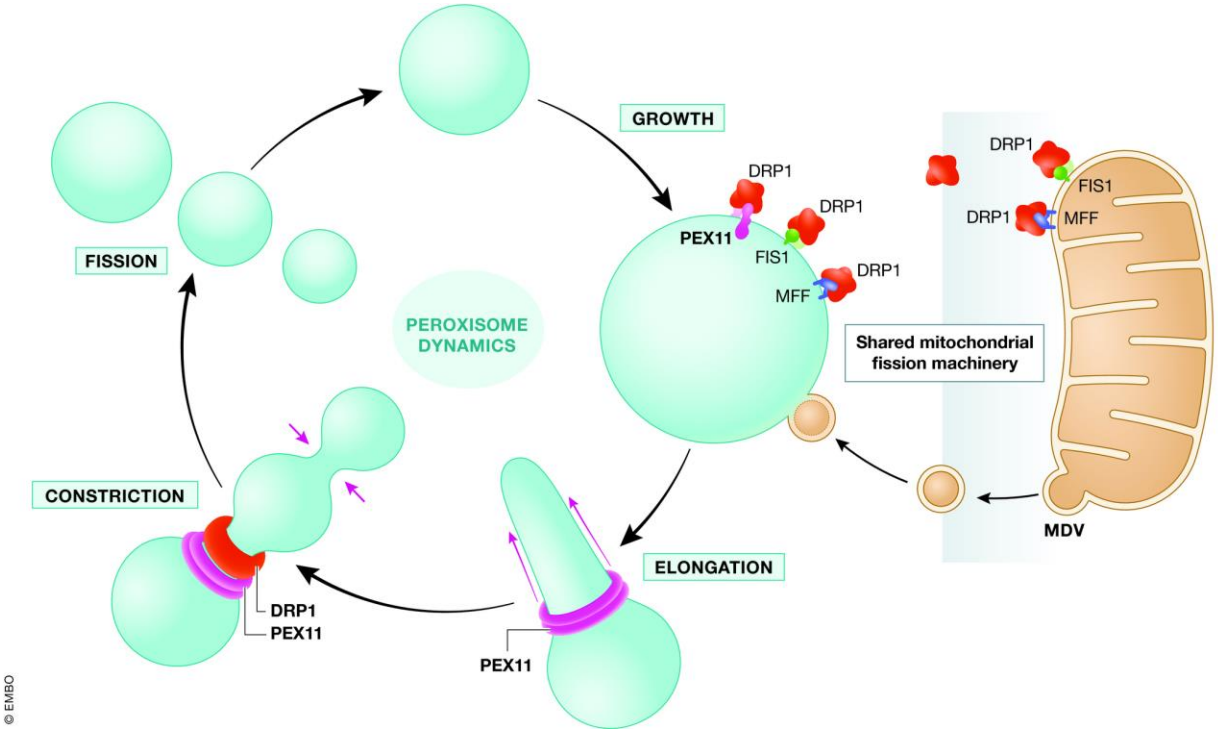

Figure 3 – Peroxisomes: Sharing Fission Machinery with Mitochondria (Sharma, A et al. 2019)

As shown in Fig. 3., Peroxisomes undergo a coordinated cycle of elongation and fission, a process akin to mitochondrial dynamics. Membrane scission, crucial for peroxisome division, involves DRP1, similar to mitochondrial fission (Sesaki H et al. 2014). Adaptor proteins FIS1 and MFF, along with PEX11, regulate peroxisome fission by orchestrating membrane constriction (Kobayashi S et al. 2007). Notably, PEX11β, belongs to the PEX11 protein family, facilitates the early fission phase by initiating membrane protrusions and recruiting DRP1 (Yoshida Y et al. 2015). The intricate interplay between peroxisome and mitochondrial dynamics, governed by shared mechanisms, underscores their intertwined roles in cellular aging.

1.3 Peroxisomes inter-organelle contact sites

1.3.1 Peroxisome-Mitochondrion-MCSs

Peroxisome-mitochondrion membrane contact sites (PO-Mito-MCSs) are essential for coordinating various cellular processes, including FA β-oxidation, ROS metabolism, and antiviral defense. The intimate physical proximity between peroxisomes and mitochondria enables the exchange of signaling molecules as well as the metabolic intermediates to occur seamlessly across these organellar structures (Fan et al., 2016). While the exact mechanisms of PO-Mito-MCS formation and function are not fully understood, studies in yeast have revealed that proteins like PEX11 and PEX34 interact with components of the ERMES complex, establishing contact sites between the two organellar structures (Mattiazzi Ušaj et al., 2015). Additionally, in mammalian cells, proteins such as PEX11β and ACBD2/ECI2 play a key role in facilitating peroxisome-mitochondrion membrane contact sites (PO-Mito-MCSs) (Fan et al., 2016). Even though, the exact mechanisms of PO-Mito-MCS formation and function are not fully understood, they likely involve the exchange of β-oxidation products and redox signaling molecules (Fransen and Lismont, 2018). Understanding the molecular mechanisms and functional significance of PO-Mito-MCSs could provide insights into cellular metabolism and disease pathology.

1.3.2 ER–peroxisome interactions

PO-ER-MCSs have a critical function in regulating lipid metabolism and maintaining cellular homeostasis. These membrane contact sites (MCSs) aid in lipid transfer, such as phospholipids and cholesterol, between ER and peroxisomes, contributing to the formation of essential cellular components. As shown in Fig. 4, ACBD5, a peroxisomal membrane protein, interacts with VAPA/B proteins located on the ER membrane, forming tethered MCSs that facilitate lipid exchange between the both organelles (Costello et al., 2017). Furthermore, the regulation of unfolded protein response is achieved through ATF6α and peroxisomal protein ABCD3 interacting at PO-ER-MCSs, demonstrating the importance of these contact sites in responding to cellular stress (Torres et al., 2019). Disruption of PO-ER-MCSs affects peroxisome dynamics and lipid metabolism, emphasizing their importance in cellular function and human health. Further research into the molecular mechanisms underlying PO-ER-MCS formation and

function may provide insights into the pathogenesis of metabolic disorders and potential therapeutic targets (Schrader et al., 2013).

1.3.3 Peroxisome-Lipid Droplet-MCSs

Peroxisome-lipid droplet membrane contact sites (PO-LD-MCSs) are vital in the coordination of lipid metabolism and maintaining cellular homeostasis. These contact sites helps transfer fatty acids (FAs) to peroxisomes from the lipid droplets (LDs), enabling β-oxidation and preventing the accumulation of lipotoxic intermediates (Kong et al., 2020). The PO-LD-MCSs formation involves tethering complexes, such as M1 Spastin-ABCD1, which promote the transport of fatty acids to peroxisomes from Lipid Droplets (Chang et al., 2019). Additionally, PO-LD-MCSs regulate lipolysis by facilitating the movement of lipases. For instance, during fasting, the transfer of adipose triglyceride lipase (ATGL) to lipid droplets occurs (Kong et al., 2020). Dysregulation of PO-LD-MCSs is linked to several physiological disorders such as hereditary spastic paraplegias and metabolic illnesses (Kong et al., 2020). Understanding the molecular mechanisms and functional significance of PO-LD-MCSs could offer insights into the pathogenesis of these diseases and identify potential therapeutic targets.

1.3.4 Peroxisome-Lysosome-MCSs

Peroxisome-lysosome membrane contact sites (PO-Lyso-MCSs) play an essential part in the movement of cholesterol within cells and maintaining cellular balance. These contact sites help move cholesterol from the lysosomes to peroxisomes, a process essential for maintaining cellular lipid balance (Chu et al., 2015). As shown in Fig. 4, the connection between PO-Lyso-MCSs relies on the presence of peroxisomal PI(4,5)P2 lipid and lysosomal synaptotagmin VII (Syt7) protein, which bind the two organelles together. (Chu et al., 2015). Dysregulation of PO-Lyso-MCSs is implicated in pathological mechanisms associated with peroxisomal disorders, leading to abnormal cholesterol accumulation in lysosomes (Chu et al., 2015). Additionally, the studies indicates that PO-Lyso-MCSs may play a part in regulating mTOR signaling when cells are under stress, but more studies are required to understand this process.

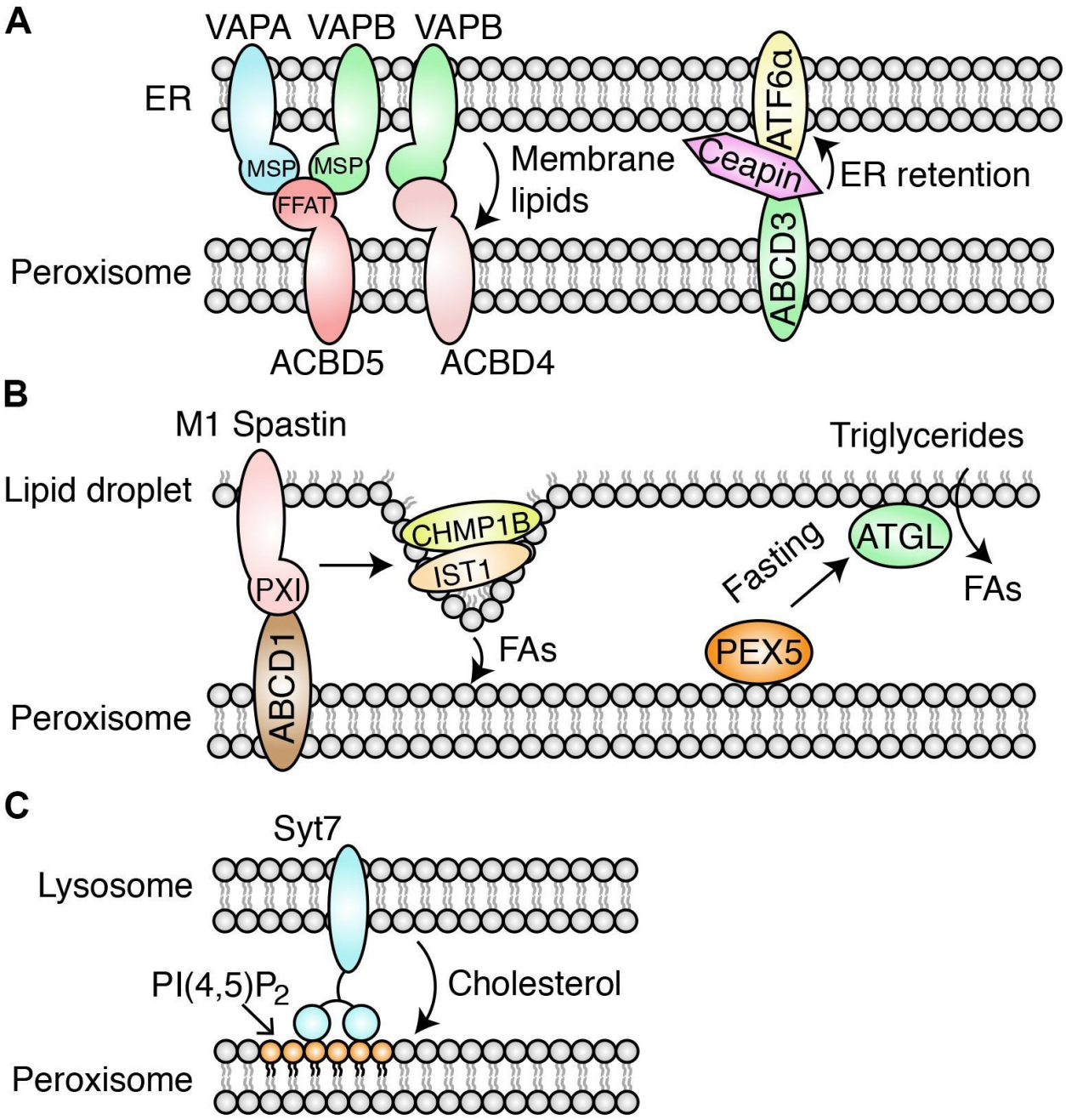

Figure 4: Peroxisome-Organelle Membrane Contact Sites (PO-MCSs) in Mammalian Cells - (A) Peroxisome-Endoplasmic Reticulum (ER) MCS: ACBD5's FFAT motif interacts with VAPA/B's MSP domain, helping move lipids from the ER to peroxisomes. Ceapin anchors ATF6α to peroxisomal ABCD3 at the ER. (B) Peroxisome-Lipid Droplet (LD) MCS: M1 Spastin binds to ABCD1, bringing IST1 and CHMP1B to LDs, facilitating fatty acid transport. During periods of fasting, PEX5 recruits ATGL to the MCS, which enhances the breakdown of triglycerides. (C) Peroxisome-Lysosome

(Lyso) contact site is enabled by PI(4,5)P2 and Syt7, which aid in transporting cholesterol from lysosomes to peroxisomes (Chen, et al. 2020).

1.4 The Role of inheritance and function of organelles in embryogenesis.

The process of embryogenesis relies heavily on the inheritance and function of subcellular organelles, which play critical roles in cellular differentiation and development. Subcellular organelles, including the ER, Golgi complex, and mitochondria, are maternally inherited and transferred to developing oocytes in both vertebrates (e.g., mice) and invertebrates (e.g., *Drosophila*). This transfer is imperative for various cellular processes during early development.

Mitochondria, in particular, serve as crucial energy generators and regulators of calcium levels within cells. In various organisms, such as *Drosophila* and Caenorhabditis elegans, mitochondria undergo elimination either before or after fertilization (DeLuca et al. 2011). Mutations in the mitochondrial genome can lead to a range of mitochondrial diseases transmitted from the mother to offspring. During embryonic development, mitochondria undergo significant morphological changes, transitioning from a small, globular state to a tubular architecture with heightened ATP-generating capacity (Chen et al. 2012). They closely interact with the other organelles such as ER and the cytoskeleton, helping with tasks such as producing ATP and regulating calcium levels (Dumollard et al. 2007).

Research has demonstrated the close connection between the arrangement of the ER and Golgi apparatus with the positioning of the nucleus and microtubules in the cell (Frescas et al. 2006). During the preblastoderm stage of a *Drosophila* embryo, the ER and Golgi membranes are specifically positioned at the outer edge of the embryo, whereas nuclei and centrosomes are situated more towards the interior of the embryo (Freeman, et al. 1986). This spatial arrangement necessitates mechanisms for partitioning ER and Golgi among nuclei to ensure equitable distribution during subsequent cellularization stages.

The localized organization of these organelles also influences gene and protein expression patterns during embryogenesis. It has been shown that the compartmentalization of ER and Golgi may facilitate the localization of maternal mRNAs

and proteins, regulating spatial and temporal gene expression patterns critical for embryonic development (Frescas et al. 2006).

Furthermore, the proper distribution and function of organelles, particularly the ER and Golgi, and mitochondria are crucial for cellularization, where the partitioning of membranes among nuclei ensures homogenous distribution and facilitates plasma membrane synthesis (Frescas et al. 2006 and Rikhy et al. 2015).

In summary, it is evident that the inheritance and function of organelles play critical roles in various cellular processes during embryogenesis. Proper organelle inheritance is vital for the development and differentiation of embryos, highlighting the intricate interplay between organelles and cellular processes during early development. Their organization and distribution, tightly regulated by cytoskeletal elements, significantly contribute to overall embryo development and differentiation. However, the peroxisome's role in the cell, in regulating these processes remains understudied. Investigating peroxisome distribution and dynamics during *Drosophila* cellularization could offer valuable insights into their role in embryonic development.

1.5 *Drosophila* Embryo: A Model System for Investigating Peroxisomal Dynamics and Function during Embryogenesis

In the *Drosophila* embryo, the mother provides the instructions for establishing the embryonic axes. Alongside patterning cues, organelles such as mitochondria, endoplasmic reticulum (ER), and Golgi complexes are inherited from the maternal source. *Drosophila* embryos offer a dynamic developmental environment, characterized by accelerated development than other systems, and are well-suited for visualization using fluorescent labels due to the presence of genetically modified markers (Mavrakis et al., 2008). Upon fertilization, the initial 13 nuclear division cycles (NC) in a *Drosophila* embryo occur synchronously. The first 9 NC cycles take place deep within the embryo's cytoplasm, a stage referred to as the preblastoderm stage where, nuclei initiate their migration towards the outer edge of the embryo and reach the cortex by the start of NC 10. Afterwards, quick divisions happen at the outer edge of the embryo, ranging from NC 10 to NC 13. During this phase, as described by Karr and Alberts in 1986a, the cells go through incomplete cytokinesis.This developmental phase is termed the syncytial

blastoderm because of the absence of complete membrane encapsulation around the nuclei. Even with this syncytial nature, organelles like the ER and Golgi complexes show specific positioning around each nucleus contributing to a compartmentalized system (Frescas et al., 2006). Proteins on the plasma membrane which are transported by Golgi complexes are not exchanged among the membranes of neighboring nuclei, delineating distinct syncytial cells (Mavrakis et al., 2009). Germ cells or pole cells represent the sole complete cells present during this phase, and are the progenitors of the future gametes and are set aside early in embryogenesis. In the interphase of NC 14, there is an ingression of the plasma membrane towards the basal side, eventually enclosing the nuclei. This process, known as cellularization, marks the formation of the first epithelial cell layer in the embryo, marking the transition from the syncytial blastoderm stage to the cellular blastoderm stage. Cellularization involves two separate stages of membrane movement: an initial slow stage followed by a rapid stage. According to research done earlier, the initial stage of cellularization includes the step-by-step positioning of acto-myosin assembly at the tips of the furrow hexagonally, causing constriction of a membrane into a circular form through the processes which are dependent on myosin. Following this, a ring is formed, tightening with actin cross-linkers, and ultimately resulting in myosin detachment, as explained by He et al. (2016), and Young et al. (1991).

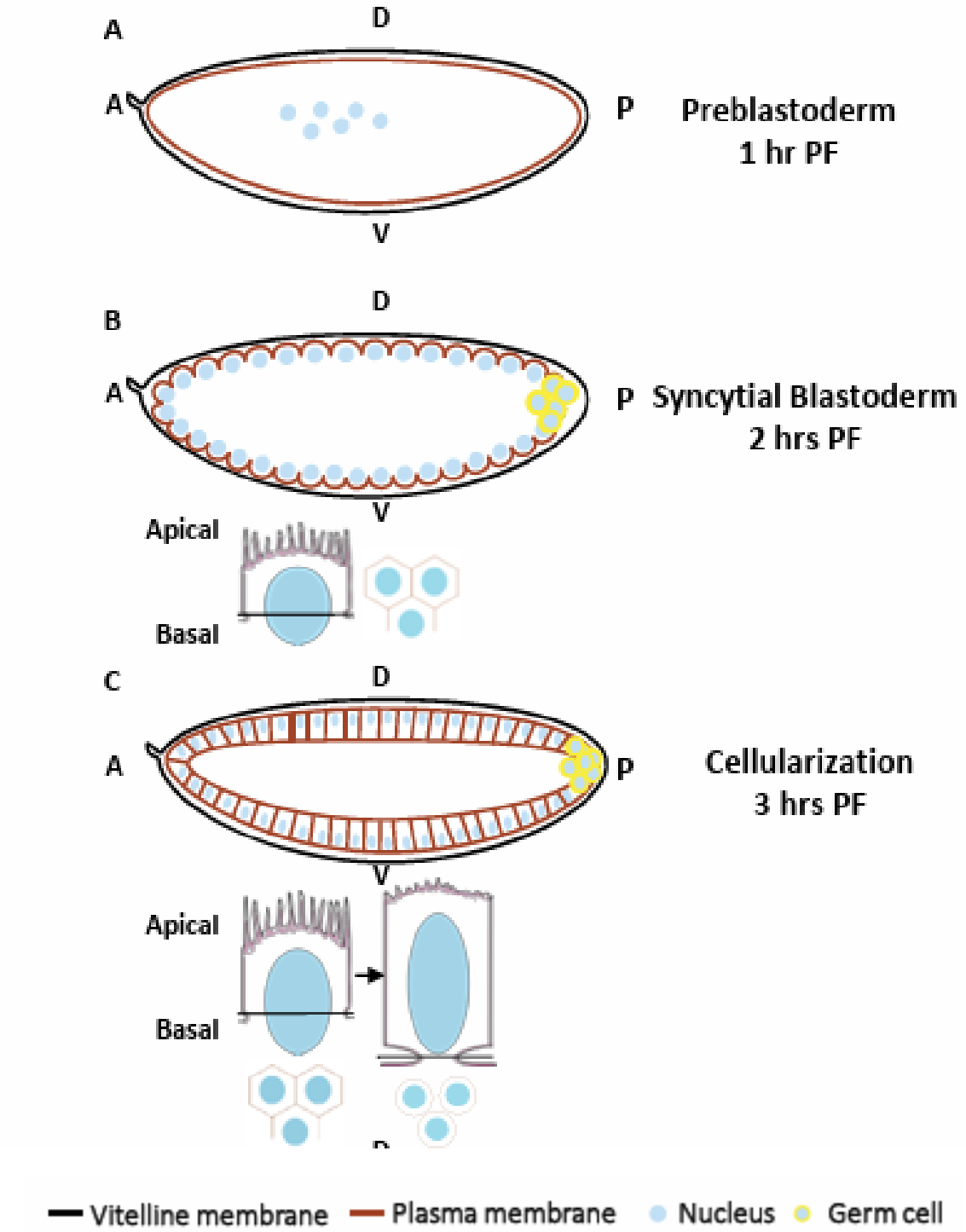
A
D
A
P
V
Preblastoderm
1 hr PF
B
D
A
P
V
Syncytial Blastoderm
2 hrs PF
Apical
Basal
C
D
A
P
V
Cellularization
3 hrs PF
Apical
Basal
Vitelline membrane
Plasma membrane
Nucleus
Germ cell

Figure 5 : *Drosophila* Embryogenesis as a Model System to probe Peroxiosmes dynamics- Following fertilization, nuclei undergo division within the embryo from NC1 to NC9 **(A).** At NC10, nuclei migrate to the periphery of the embryo and experienced synchronous divisions until NC13 **(B).** Sagittal schematics illustrate the apical coverage of nuclei by the plasma membrane, with a zoomed-in view revealing a hexagonal arrangement of cells at membrane tips (dashed black line) **(B).** During cellularization at NC14, membranes ingress to completely enclose the nuclei **(C).** Basal sections, indicated by black dotted lines in sagittal views, depict a transition from hexagonal geometry to circular shape morphology as the membrane undergoes constriction **(C).** (adapted from Sayali's thesis)

1.6 Objectives of the project -

Embryogenesis requires the coordinated function of organelles for various processes of epithelial-like cell formation and patterning. Appropriate positioning and function of mitochondria have been recently shown to be important for cell formation and cell remodelling (Chowdhary et al. 2020). Even though understanding of the various roles played by peroxisomes has expanded over time, more explanation is still needed regarding their impact on governing the different stages of cell formation and remodeling. This project embarks on a journey to unravel the mysteries surrounding peroxisomes' involvement in *Drosophila* embryogenesis. We aim to elucidate the distribution and dynamics of peroxisomes in the context of epithelial-like cell formation by live imaging and fixed immunostaining using markers specific to mature peroxisomes. In various systems, Drp1 has been demonstrated to play a role in splitting of mitochondria and peroxisomes. Previous studies in the lab have shown the role of Drp1-mediated fission of mitochondria in the migration of mitochondria and the formation of the cell during *Drosophila* embryogenesis. We will determine if Drp1 is required for peroxisomal fission during these processes. Intriguingly, we will further elucidate their change in distribution in embryos containing a defect in the Drp1 protein.

Mitochondrial fission has been correlated with an appropriate level of reactive oxygen species for regulated cell formation in *Drosophila* embryogenesis. We will explore if peroxisomal dynamics play a similar role and their distribution is affected by levels of reactive oxygen species in the cytoplasm and mitochondria in *Drosophila*

embryogenesis. We will test the role of peroxisome homeostasis in regulating the cellular response to reactive oxygen species in embryogenesis.

Furthermore, in our quest to decipher the intricate crosstalk between peroxisomes, mitochondria, and ROS levels, we will delve into the mechanisms governing peroxisome biogenesis. Peroxisome biogenesis in *Drosophila* is a complex process controlled by a group of peroxin (PEX) proteins. The 15 PEX genes in the *Drosophila* genome encode proteins responsible for targeting, organizing, and catalyzing reactions within peroxisomes (Mast et al., 2011). PEX proteins are essential for the formation of peroxisomes in *Drosophila* as they facilitate the creation of the peroxisomal membrane, the import of matrix proteins, as well as the division of peroxisomes. These PEX proteins work together to ensure that peroxisomes are properly assembled and functioning.

In summary, this project aims to comprehensively analyze the distribution, dynamics, and functional significance of peroxisomes during the early stages of embryogenesis in *Drosophila*. It seeks to shed light on the formation and functional roles of peroxisomes in the intricate processes of embryonic development.

Aims of the project:

1. To elucidate the distribution and dynamics of peroxisomes during epithelial-like cell formation in *Drosophila* embryogenesis by live imaging and fixed immunostaining.
2. To identify the role of the Pex genes in Peroxisomes biogenesis.
3. To study the change in distribution and morphology of peroxisomes in Drp1 mutant embryos in *Drosophila* cellularization.
4. To test if peroxisome distribution is affected by levels of reactive oxygen species in the cytoplasm and mitochondria in *Drosophila* embryogenesis.

Chapter 2 Materials and Methods

1. ***Drosophila* stocks and genetics**

All Fly stocks were maintained at a temperature of 25°C in the standard corn meal agar medium. Stocks were obtained from Snehal (fly lab facility, IISER Pune) or Bloomington *Drosophila* Stock Center (BDSC). All RNAi lines were activated using maternally expressed nanos-Gal4 at a temperature of 28°C to study the effect on peroxisomes numbers and dynamics. The flies for the crosses with required genotypes were selected with the help of their respective balancers. The selected F1 flies were introduced into the cages for the embryo collection having yeast paste supplemented with 3% sucrose-agar media and kept at a temperature of 28°C.

Table 1 - List of the fly stocks used in this study-

Fly stocks	Source/References
pUASP-SKL-RFP (t65 RR/1/46)	Peter Kim and Richa Rikhy JLS lab,
UAS-SKL-RFP/Cyo; NG4	- Generated by recombining nanos-Gal4 and UASP-SKL-RFP
Nanos-Gal4	Bloomington Stock #4937
UAS-*pex1* RNAi	Bloomington Stock #51497
UAS-*pex3* RNAi	Bloomington Stock #50694
UAS-*pex5* RNAi	Bloomington Stock #42854
UAS-*pex7* RNAi	Bloomington Stock #76994
UAS-*pex10* RNAi	Bloomington Stock #51826
UAS-*pex11a/b* RNAi	Bloomington Stock #42883
UAS-*pex12* RNAi	Bloomington Stock # 53308
UAS-*pex13* RNAi	Bloomington Stock #50697
UAS-*pex14* RNAi	Bloomington Stock #77180
UAS-*pex16* RNAi	Bloomington Stock #57495
UAS-*pex19* RNAi	Bloomington Stock #50702
UAS-*pex23* RNAi	Bloomington Stock #34370
UAS-*sod2* RNAi	Bloomington Stock #25969
pUASp-Drp1^{SG}	Generated in the lab
UAS-Drp1^{SG}; *sod2* RNAi	Generated in the lab (Somya)
UAS-Vdac RNAi	Bloomington Stock #67873

Fly stocks	Source/References
UASP-Tubulin-GFP	Richa Rikhy (RR/0/51)

2. **The Gal4-UAS system** was used to induce the expression of transgenic (or fluorescently tagged) lines UASp-SKL-RFP. Many Gal4 driver lines are available that drive expression in specific tissues and at specific developmental times. To study the cellularization, nanos Gal4 was used which drive expression during oogenesis and allow maternal dumping of proteins in the egg for the initial stages of embryogenesis. F1 flies containing the desired genetic combination were utilized to obtain embryos, ensuring the inheritance of maternally derived phenotypes in the early embryonic stage.

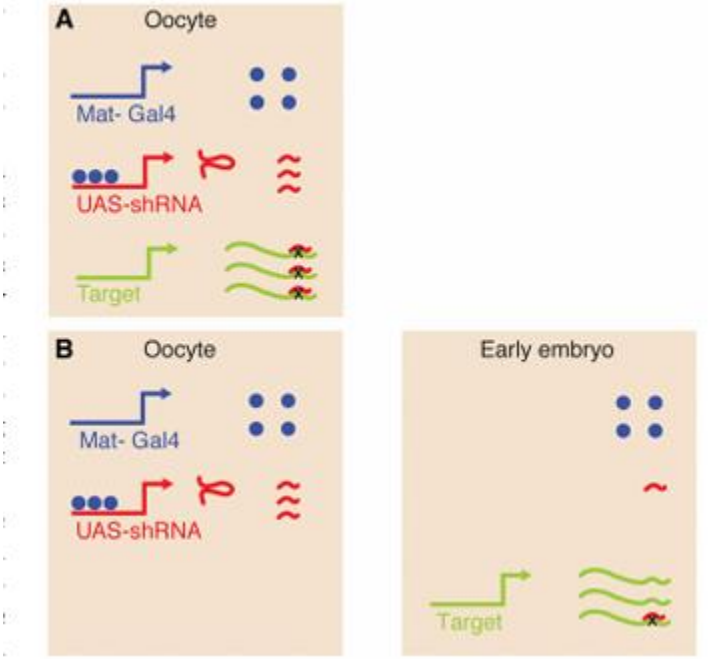

Figure 6 - Genes in embryos are knocked down through the utilization of maternally expressed Gal4 driver (depicted in blue). Gal4 expression occurs within the oocytes, thereby initiating the production of UAS-shRNA (depicted in red). This UAS-shRNA binds to and reduces the levels of target transcripts (depicted in green) that are maternally expressed within the oocyte itself (A). Furthermore, zygotic transcripts are diminished through the presence of maternally expressed UAS-shRNA that is deposited in the embryos (B). Adapted from the study conducted by Staller et al. in 2013.

3. Embryo Immunostaining

F1 flies of the desired genotype were introduced into the cages containing yeast paste supplemented with 3% sucrose-agar plates for the embryo collection. Embryos aged between 3 to 3.5 hours were then obtained for the cellularization stage. After this, the embryos were washed using distilled water to remove the yeast paste, and, then the bleaching was performed for 1 minute time period to remove the chorion layer of the embryo. Then, the fixation step was performed using the 1:1 ratio of heptane and 8% paraformaldehyde (PFA) solution in phosphate buffered saline (PBS -137 mM NaCl, 2.7 mM KCl, 10 mM Na2HPO4 and 1.8 mM KH2PO4) for approximately 25 minutes and then, hand devitellinized to remove the vitelline membrane via using insulin needles. After devitellinization, the embryos were washed for three times using PBS-T (Triton X-100, 0.3%) solution. Then, the blocking was done for 1 hour using 2% BSA solution, then, overnight treatment was done for primary antibody with dilution in 2% BSA at 4 degree. Then, on the next day, i.e after 14-16 hours, the three PBST washes is done for 5 minutes each, then, the secondary fluorescent molecular probe was diluted in PBST and added to the embryos, which were then kept for the incubation at room temperature under dark conditions for 45 mins. Subsequently, the embryos underwent 3 PBST washes. During the second wash, the nuclear stain Hoechst (1:1000 dilution) was added. Finally, the embryos were mounted on slides using Slowfade Gold.

Table 2 - List of antibodies and fluorescent probes

Antibody/Probe name	Source	Host Species	(Ab) Dilution/Concentration
Hoechst 33342	Molecular Probes	N/A	1:1000
Phalloidin,488,568	Molecular Probes	N/A	1:500
Streptavidin 488,568,633	Molecular Probes	N/A	1:500
Anti-SKL antibody	Richard Rachubinski, University of Alberta	Rabbit	1:500
Anti-Calnexin	Primary antibody	Mouse	1:100

Antibody/Probe name	Source	Host Species	(Ab) Dilution/Concentration
Secondary antibody 488,568,633	Alexa Flour	Raised in Rabbit/Mouse	1:1000

4. Embryonic lethality estimation

Embryos aged 3 hours were collected from cages containing 3% sucrose agar supplemented with yeast. Subsequently, the embryos were arranged in a 5 × 5 array (totaling 5 grids) on the fresh 3% sucrose agar plates, and then, incubated at 28 degree temperature in which the fly cage was kept. After 24 hrs of incubation, the counting was done for the embryos which were unhatched and represented as a percentage.

5. Live Imaging

The embryos, aged between 1.5 to 2 hours, were harvested from the cages and subjected to a gentle wash using distilled water. Following this, the embryos underwent dechorionation by exposure to 100% bleach for a duration of 1 minute, after which they were rinsed extensively with distilled water and dried completely using a soft tissue. The embryos were then mounted on LabTek chambers and 1X PBS was added to the chamber.

6. Microsocpy

Fixed samples were imaged using a Zeiss LSM 780 confocal laser scanning microscope equipped with a Plan Apochromat 63X/1.4 NA oil immersion objective. The frame size was set to 70.3 µm X 70.3 µm using a zoom factor of 1.92 at a resolution of 512x512 pixels. Imaging was performed in sequential mode, capturing z-stacks channel by channel. To ensure optimal image quality, the scan speed was set to 8, and an averaging of 2 was applied. Fluorescence intensity was carefully regulated to stay within the dynamic range of 255 on an 8-bit scale, utilizing the range indicator mode to prevent over-saturation of pixels. For both fixed and live samples, images were acquired from the apical to basal side with a 1 µm interval between each slice. Additionally, a 1-minute gap was maintained between each time point during live sample imaging to minimize

phototoxicity (or bleaching). To maintain a constant temperature of 25°C for live sample imaging, an incubator was utilized throughout the imaging process.

7. Image Analysis and Quantification

Image analysis consisted of fluorescence intensity measurements, membrane length and numbers quantification. All the quantification was done using ‘Image J software’ and ‘GraphPad Prism’ was used for plotting graphs and data analysis. To assess the total number of peroxisomes and their distribution throughout the Z-stack, we employed the "3D Object Counter" tool in ImageJ. It helped in determination of each peroxisome centroids after thresholding, allowing us to quantify peroxisome numbers accurately.

Quantification procedures were carried out as follows:

1. Background Subtraction:
    - Images were imported into ImageJ.
    - Background subtraction was performed using the "Subtract Background" function under "Process." A rolling ball radius of 5 pixels was applied to reduce background pixel intensity.
2. Thresholding:
    - Thresholding was conducted using the Shift + T command to ensure optimal capture of particles across all slices.
    - The thresholded image was created, and options for generating a new stack and selecting a black background for binary masks were chosen.
3. Particle Counting in 3D:
    - The 3D Counter plugin was utilized to count particles in three dimensions on the mask image that was generated after applying thresholding.
    - Note that - as our imaging was conducted at a 1µm step size, individual peroxisomes typically spanned 2 to 3 planes. The 3D Counter provided a centroid map of all particles along with their corresponding statistics.
4. Particle Analysis:
    - The centroid map was thresholded to count particles in 3D space.

- The "Analyze Particle" function was employed to obtain statistics on the number of particles present in each plane.

This methodology enabled precise quantification of peroxisome numbers within the specified volume, essential for our experimental analyses.
Furthermore, with the obtained data utilized to determine average apical number and size, providing valuable insights into peroxisome distribution and morphology.

8. Cloning

Construction of pUASP-PAGFP-SKL Transgenic Vector -
The pUASP-PAGFP-SKL construct was designed to incorporate the peroxisomal targeting sequence (SKL) fused to Photoactivatable Green Fluorescent Protein (PAGFP) within the pUASP vector. The SKL sequence, comprising Serine, Lysine, and Leucine amino acids, was chosen for its peroxisome-targeting capabilities.

Primer Design and PCR Amplification
Primers were designed to amplify the PAGFP sequence from the PAGFP vector DNA. The forward primer was designed to overlap with PAGFP and feature overhangs compatible with the pUASP vector and the reverse primer contained the SKL sequence. Temperature Gradient PCR optimization was conducted, followed by bulk PCR using Q5 DNA Polymerase.

Primer Type	Sequence
Forward	CCGCATAGGCCACTAGTGGATCTGGTACCATGGTGAGCAAGGGCG
Reverse	AACGTTCGAGGTCGACTCTAGAGGATCCTTACAGCTTGCTCTTGTACAGCTCGTCCATGCCG

Gel Electrophoresis and Purification -
PCR products were analyzed via gel electrophoresis to verify the presence of the desired DNA band. Gel extraction and purification methods were employed to isolate the amplified PAGFP-SKL sequence.

Sequencing and Gibson Assembly -

The purified PAGFP-SKL sequence, with overhangs of the pUASP vector, underwent sequencing to confirm accuracy. Gibson assembly was performed to ligate the PA-GFP-SKL sequence into the pUASP vector.

Transformation and Plasmid Purification -

The ligated construct was transformed into bacterial cells (DH5α cells) using ampicillin as a selectable marker. Transformed colonies were selected, and the plasmid containing the transgenic gene construct was purified using midiprep.

Microinjection into *Drosophila* Embryos -

The purified pUASP-PAGFP-SKL vector having concentration (1ug/ul) was sent to the NCBS injection facility in Bangalore, India, for microinjection into *Drosophila* embryos. The NCBS injection facility will conduct the injection process and subsequent selection of transgenic animals.

Chapter 3 Results

3.1 Peroxisomes accumulate in the apical region with the progression of cellularization in *Drosophila* embryogenesis (fixed and live imaging).

The distribution and organization of peroxisomes in *Drosophila* cellularization embryos is visualised by staining with the anti-SKL antibody **(Figure7)** that binds to the SKL tag found on peroxisomal proteins and hence, allows to visualize peroxisomes via immunostaining by detecting the presence of the SKL tag through specific fluorescence or color markers. The data shows that peroxisomes appear as very small and punctae-like structure during cellularization and they are present basally during early cellularization and as cellularization proceed peroxisomes start migrating apically and there is an overall increase in apical peroxisomes.

Furthermore, we visualized peroxisome distribution at different stages of cellularization in embryos using two distinct peroxisome markers: GAL4-driven UASp-SKL-RFP (Red) and anti-SKL immunostaining (Green) **(Figure 8).** SKL-RFP is a fusion protein where the SKL tag guides RFP (Red Fluorescent Protein) to peroxisomes, allowing the visualization of peroxisomes in live or fixed cells through the red fluorescence emitted by RFP. The merged sections displayed a significant overlap of SKL-RFP and anti-SKL tags, indicating that both markers are reliable for peroxisome visualization.

It is important to note that the SKL-RFP signal is can be clearly seen at the basal region in saggital sections of the embryos **(Figure 8)**. However, the intensity of the anti-SKL staining in basal sections is comparatively lower, indicating a potential issue with antibody penetration.

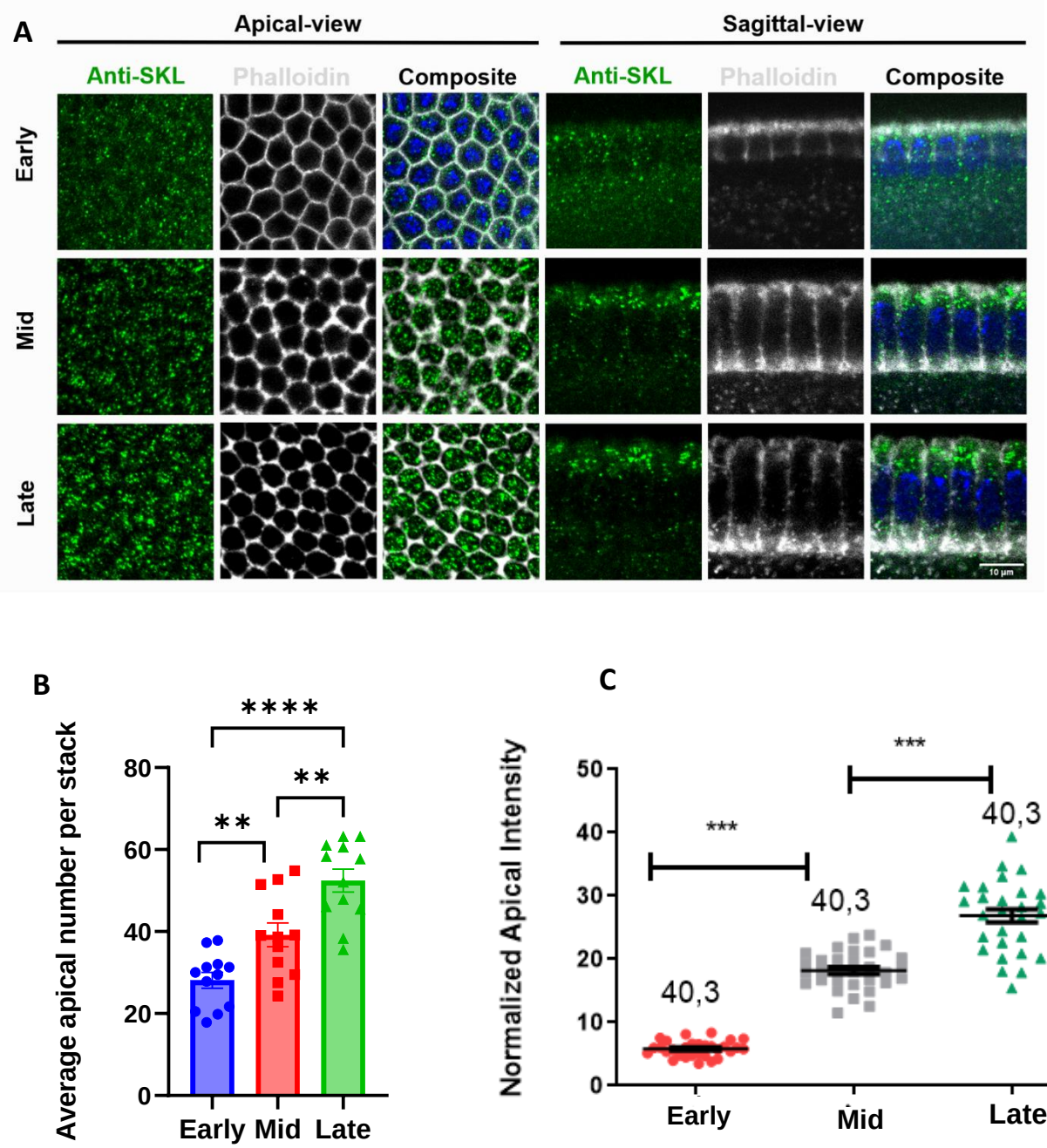

Figure-7. Apical Peroxisomes number increases during *Drosophila* cellularization. Peroxisome is marked with anti-SKL(Green), membrane is marked with Phalloidin (Gray), and, composite section showing the membrane and peroxisomes together apically and sagittally in Early, Mid and late cellularizing embryo. Scale bar is 10µm **(A)**. The average apical number of peroxisomes per section gradually increases from the Early (blue, B) to Mid (red, B) and Late (green, B) stages of cellularization. This was quantified from n = 3 embryos for each stage, with four sections of 34.2 * 34.2 µm from each embryo **(B).** Additionally, the normalized peroxisomal apical intensity per stack

also increases with the progression of cellularization **(C).** The data is represented as mean ± SEM, with significance levels denoted as follows: * for $p < 0.05$, ** for $p < 0.01$, *** for $p < 0.001$, and **** for $p < 0.0001$. These values were determined using a two-tailed Mann-Whitney test.

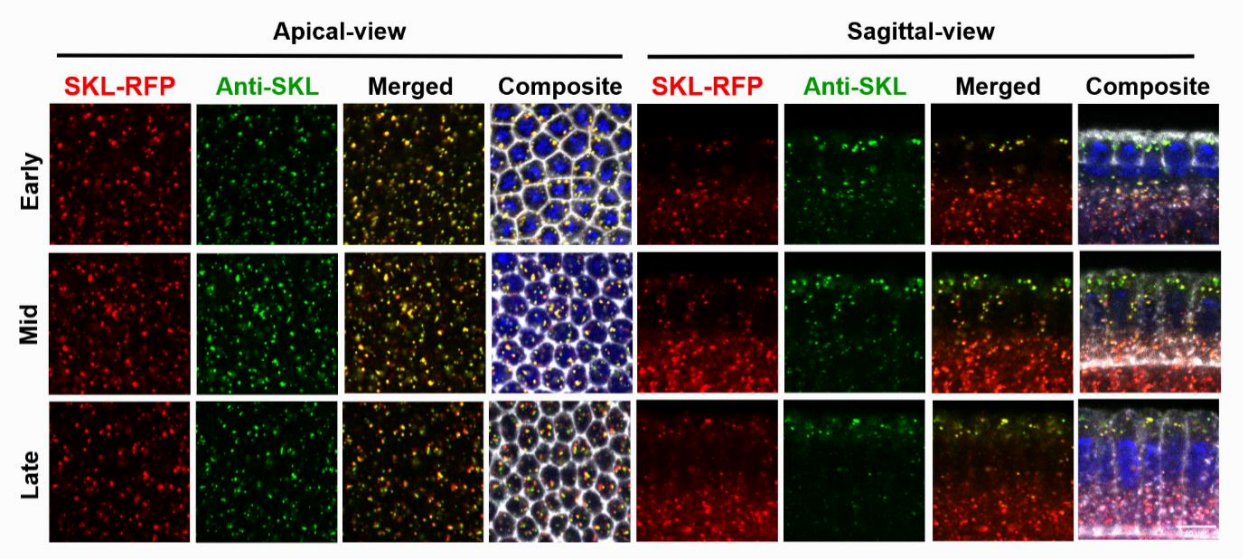

Figure-8. **Distribution of peroxisomes in early, mid, and late cellularizing embryo using two imaging tools**. Peroxisomes were visualized using GAL4 driven UASp-SKL-RFP tag (Red) and anti-SKL antibody (Green). Merged images illustrate the overlap of both SKL-RFP and anti-SKL signals, indicating potential co-localization. Additionally, composite sections were generated, demonstrating the localization of membrane (labeled with phalloidin in Gray), nucleus (stained with Hoechst dye), and the combined signal of SKL-RFP and anti-SKL. Scale bar is 10µm.

- **Peroxisomal Repositioning: Basal to Apical Translocation During *Drosophila* Cellularization.**

To examine the peroxisomal distribution and dynamics during *Drosophila* cellularization, we also performed the live imaging in addition to fixed immunostaining of the embryos at the temperature of 25°C expressing both SKL-RFP and Mito-GFP fluorescence tags **(Figure 9A and 9B)**. During the process of cellularization, we analyzed three distinct time points for the quantitative analysis of the distribution of peroxisomes: the initial phase (early, ~4 min), the intermediate phase (mid, ~20 min), and the final phase (late, ~42 min). The SKL-RFP fluorescence mean intensity as well as peroxisome numbers were quantified across apical to basal sections of the embryos, with a 1 µm depth increments **(Figure 10A and 10B)**. The results from the living imaging showed the

similar increase as seen in the fixed immunostaining of the SKL-RFP fluorescence intensity as well as the numbers in the apical region and in addition to that, the decrease in the basal intensity is also clearly visible during the progress of cellularization **(Figure 10A)**. We can clearly observe from both the graphs of fluorescence SKL-RFP mean intensity and numbers that at initial time point i.e. at the early stage, there is a highest peak at the basal region, and at the mid stage of cellularization, there is the reduction in the basal peak intensity and increment in the apical peak intensity and, finally at the late stage of cellularization, there is the single peak in the apical region of the embryo **(Figure 10A and 10B)**. We also quantified the average apical number of peroxisomes per stack **(Figure 10C)** as well as the average basal number of peroxisomes per stack **(Figure 10D)** across different stages of cellularization. The data showed the same result that during early cellularization, there is an apically increase and basally decrease in the peroxisomes numbers with the progress of cellularization. We also plotted the total number of peroxisomes **(Figure 10E)** normalized to a maximum at early, mid, and late stages, which shows no or insignificant biogenesis happening through the cellularization. Hence, indicating that there is likely the migration of peroxisomes with the progress of cellularization from basal to apical side as similar to mitochondria, which has been shown in our lab previously (Chowdhary et al., 2020).

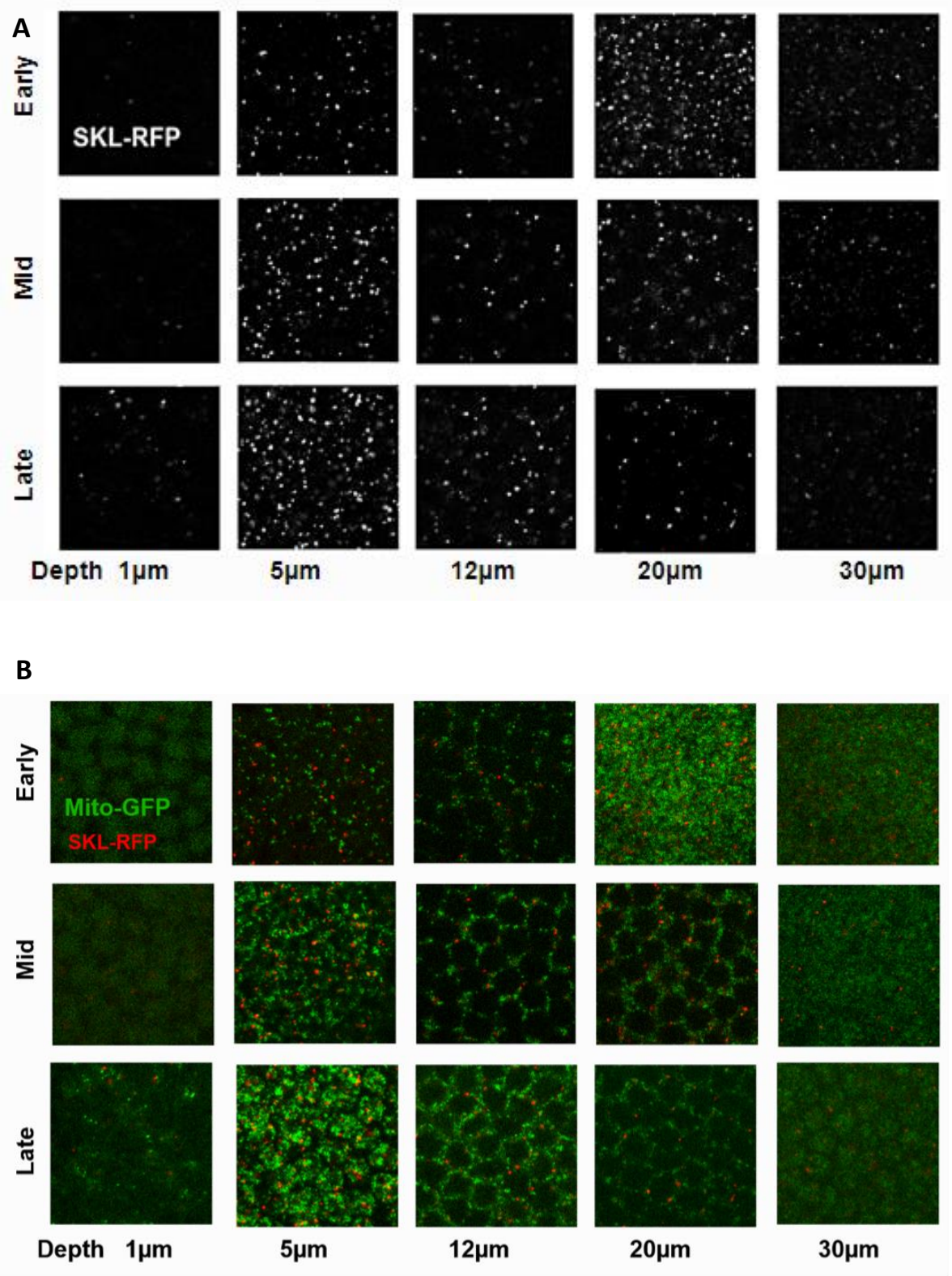

Figure-9 Apical translocation of Peroxisomes during *Drosophila* cellularization. The distribution of peroxisomes **(A)** and composite **(B)** showing Mitochondria and Peroxisomes together

different stages of cellularization. The peroxisome is marked with a GAL4-driven UASp-SKL-RFP tag (red), and, Mitochondria is marked with a Mito-GFP tag(green). Images captured from the live imaging of these embryos is represented at various depths, ranging from 1 µm to 30 µm for different stages of cellularization. Interestingly, a noticeable increase in the fluorescence intensity for both SKL-RFP and Mito-GFP was observed at the 5 µm depth (apical region of the embryo) with the progress of cellularization.

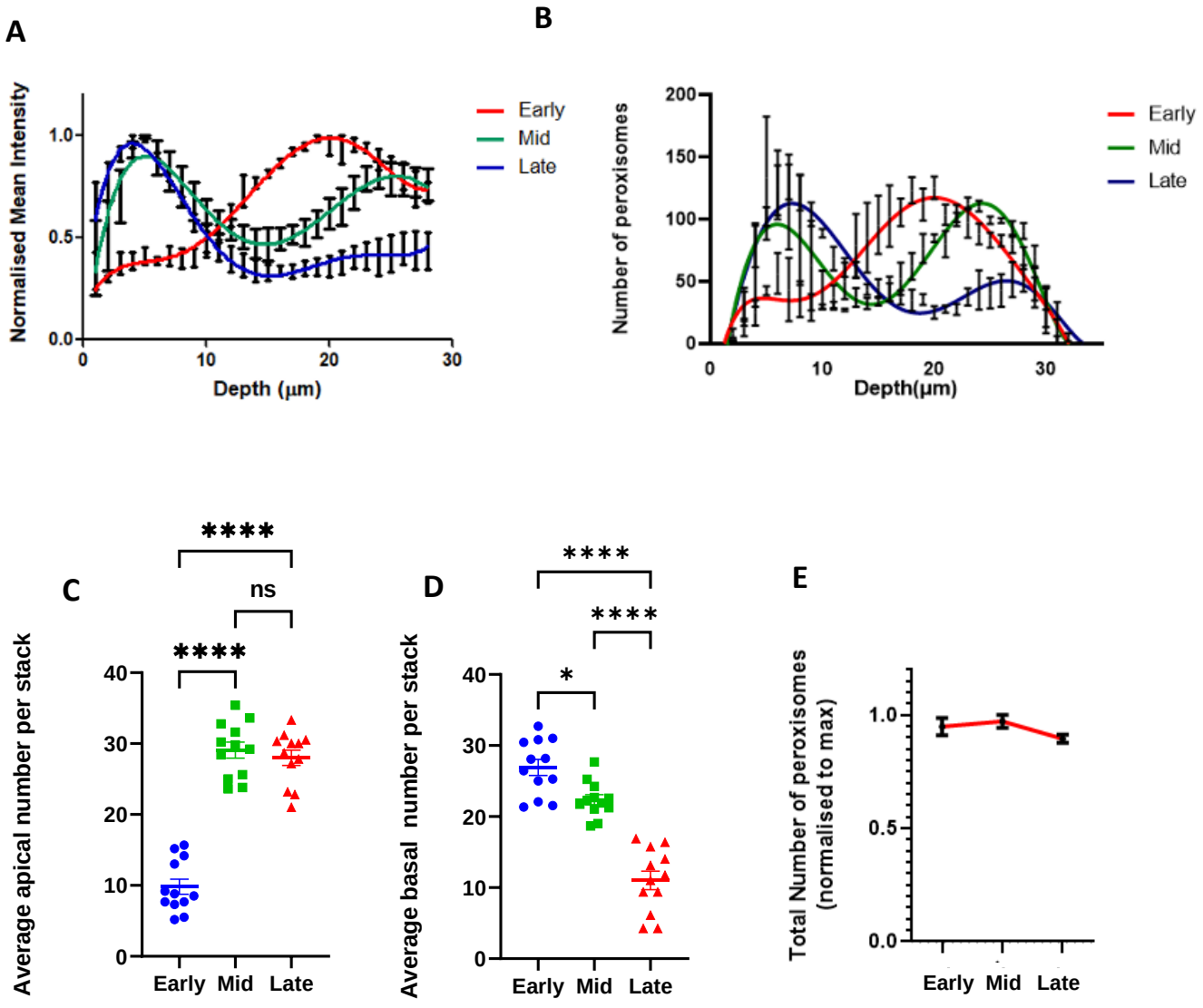

Figure-10 The peroxisomes distribution across different stages of cellularization (live imaging analysis). The graph in **(A)** displays the SKL-RFP (red) fluorescence mean intensity which

is quantified across various depths with 1 µm increments and plotted for different stages of cellularization i.e, Early (Red), Mid (Green), and Late (Blue); n = 3 embryos. **(B)** Shows the number of peroxisomes at different depths during cellularization.. **(C)** Represents the increase in the average apical number of peroxisomes per stack, and **(D**) Displays the decrease in the average basal number of peroxisomes per stack with the progress of cellularization. Finally, **(E**) presents the total number of peroxisomes normalised to the maximum at each stage of cellularization . The data is represented as mean ± SEM, with significance levels denoted as follows: * for $p < 0.05$, ** for $p < 0.01$, *** for $p < 0.001$, and **** for $p < 0.0001$. These values were determined using a two-tailed Mann-Whitney test.

Aim 3.2 - To investigate the role of PEX proteins in the formation of peroxisomes

To study the effect of embryonic viability in the PEX mutants, we did a lethality assay in both control and some of the PEX mutants. and we see not much percentage of embryonic lethality in PEX mutants as compared to control. The **table 3** below summaries the data.

Peroxisomes formation proteins which are depleted	Lethality(28°C)	Peroxisomes present or not
WIII8(control)	~6%	----------control—--------
Pex1i	To be checked	No change in no. of peroxisomes
Pex5i	~10%	No change in no. of peroxisomes
Pex11i	To be checked	No change in no. of peroxisomes
Pex12i	To be checked	No change in no. of peroxisomes
Pex14i	To be checked	No change in no. of peroxisomes
Pex23i	To be checked	No change in no. of peroxisomes
Pex10i	~5%	No change in no. of peroxisomes
Pex19i	~13%	Lower no. of peroxisomes
Pex3i	~25%	Lower no. of peroxisomes
Pex16i	~8%	Absence of peroxisomes
Pex13i	~16%	Absence of peroxisomes

Table 3 – represents the lethality assay of the embryos

3.2.1 Absence of Peroxisomes upon knockdown of PEX13 and PEX16 proteins in *Drosophila* cellularization.

To investigate the impact of PEX proteins on peroxisome formation and organization, we employed RNA interference (RNAi) to inhibit PEX13 and PEX16 expression in *Drosophila* embryos using nanos-Gal4 driver, then analyzed the embryos with fixed imaging techniques.The outcomes were striking, as embryos expressing RNA interference (RNAi) against PEX 13 and PEX16 exhibited a complete absence of peroxisomes, with only a cytoplasmic signal observed **(Figure 11).** These results suggest that the downregulation or knockdown of these specific PEX proteins severely disrupts the formation and maintenance of peroxisomes, leading to the observed absence in the cellular environment. Hence, clearly indicating the role of the involvement of PEX 13 and PEX16 in the biogenesis of peroxisomes.

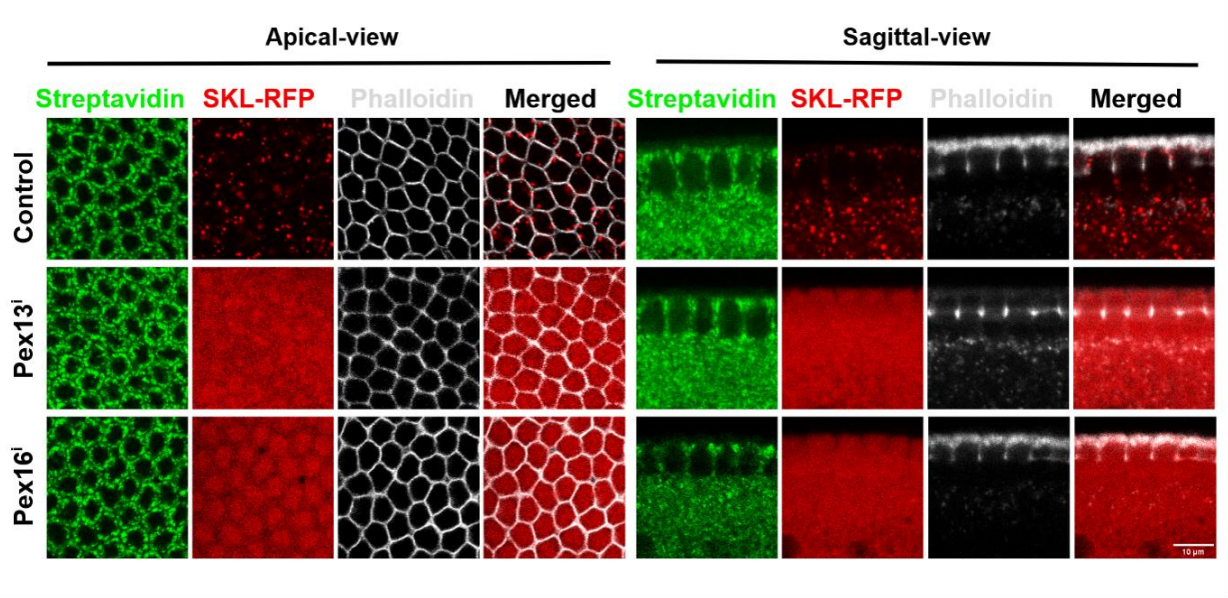

Figure-11. Absence of peroxisomes in *pex13* and *pex16* RNAi expressing embryos. Mitochondria is marked with Streptavidin (Green), Peroxisome is marked with GAL4 driven UASp-SKL-RFP tag (Red), membrane is marked with phalloidin (Gray), and composite section showing Phalloidin and SKL-RFP together. Scale bar is 10µm.

3.2.2 Decrease in Peroxisomes Number Upon Knockdown of PEX19 and PEX3 Protein in *Drosophila* cellularization.

To investigate the impact of PEX19 protein on peroxisome biogenesis and morphology, we employed RNA interference (RNAi) to inhibit PEX19 and PEX3 protein expression in *Drosophila* embryos using nanos-Gal4 driver, then analyzed the embryos with fixed imaging techniques. Our findings revealed a notable decrease in peroxisome numbers, with concurrent observation of cytoplasmic signals **(Figure 12)** in embryos expressing RNAi against PEX19. Hence, clearly indicating the role of the involvement of PEX19 protein in the biogenesis of peroxisomes.

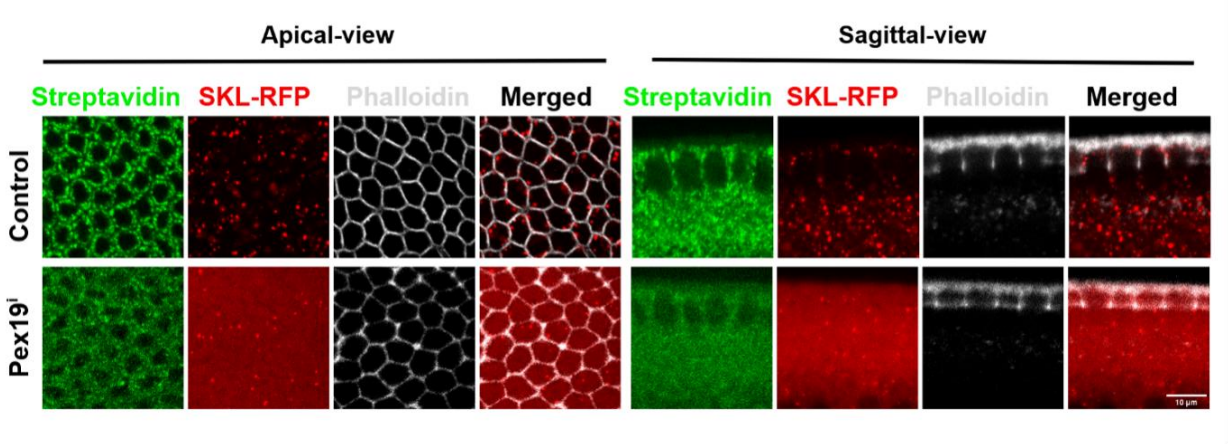

Figure-12- Decreased number of peroxisomes in *pex19* RNAi expressing embryos. Mitochondria is marked with Streptavidin (Green), Peroxisome is marked with GAL4 driven UASp-SKL-RFP tag (Red), membrane is marked with phalloidin (Gray), and composite section showing Phalloidin and SKL-RFP together. Scale bar is 10µm.

In *pex3* RNAi expressing embryos, the results depicted in **Figure 13 A** suggest that depletion of PEX3 protein in *Drosophila* embryos leads to notable changes in peroxisome dynamics during cellularization. Interestingly, despite the observed changes in peroxisome size, there was no notable changes observed in the peroxisome's count in the apical region per section across early (blue), mid (red), and late (green) stages of cellularization **(Figure 13 B)**. However, a reduction in the average apical peroxisome's number per stack was noted in *pex3*^{i} expressing embryos compared to controls throughout each stage of cellularization **(Figure 13 C)**.

The observed enlargement in peroxisome size **(Figure 13 D)** and reduction in peroxisome count in *pex3*^{i} embryos aligns with our understanding of PEX3's role in peroxisome biogenesis. PEX3 plays a role in the initial phases of peroxisome development, specifically in guiding and placing peroxisomal membrane proteins (PMPs) into the peroxisomal membrane. PEX3 depletion likely probably interferes with this mechanism, resulting in the production of a fewer peroxisomes with enlarged sizes. This aligns with earlier research indicating that perturbations in PMP targeting or insertion can result in abnormal peroxisome morphology.

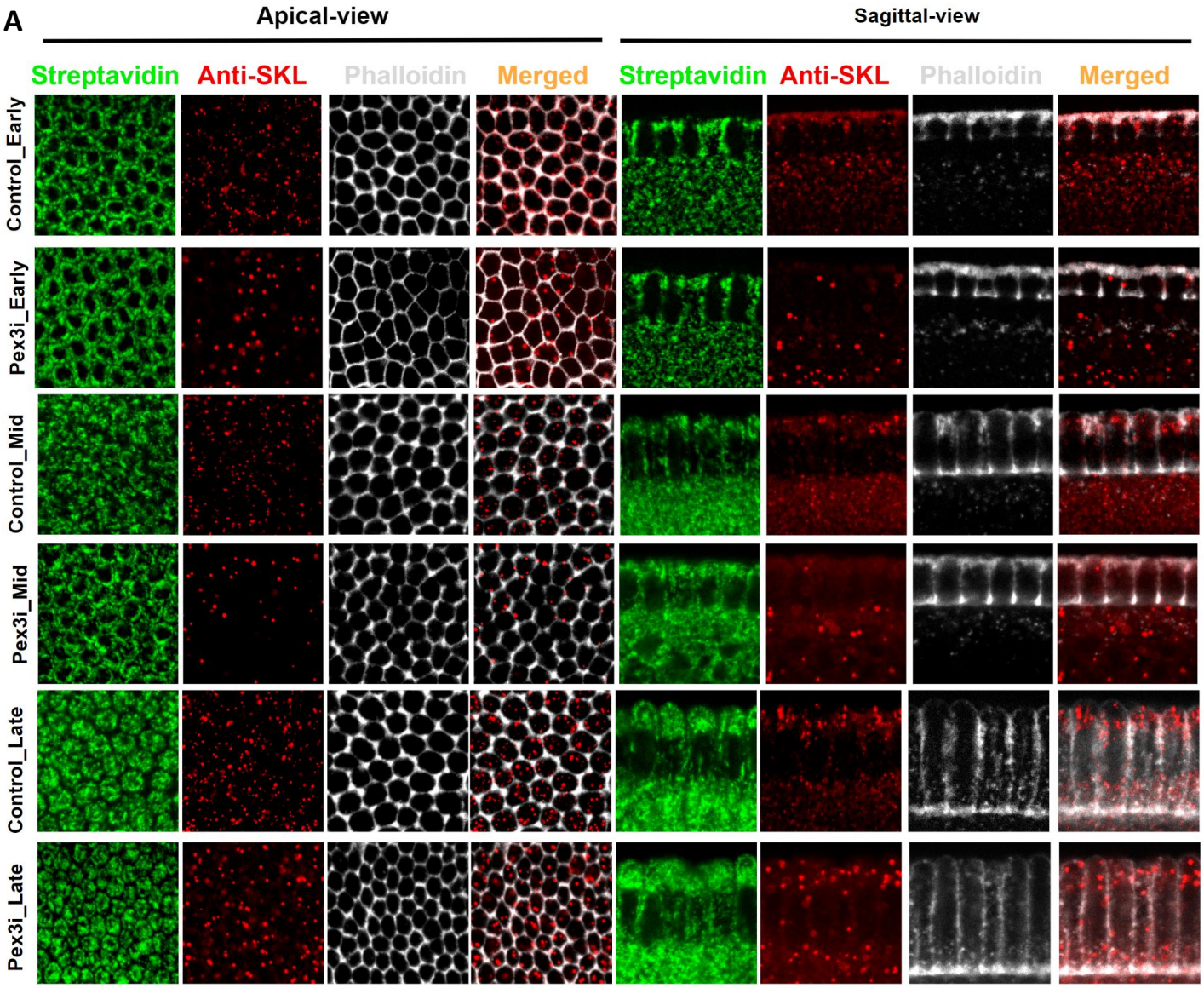

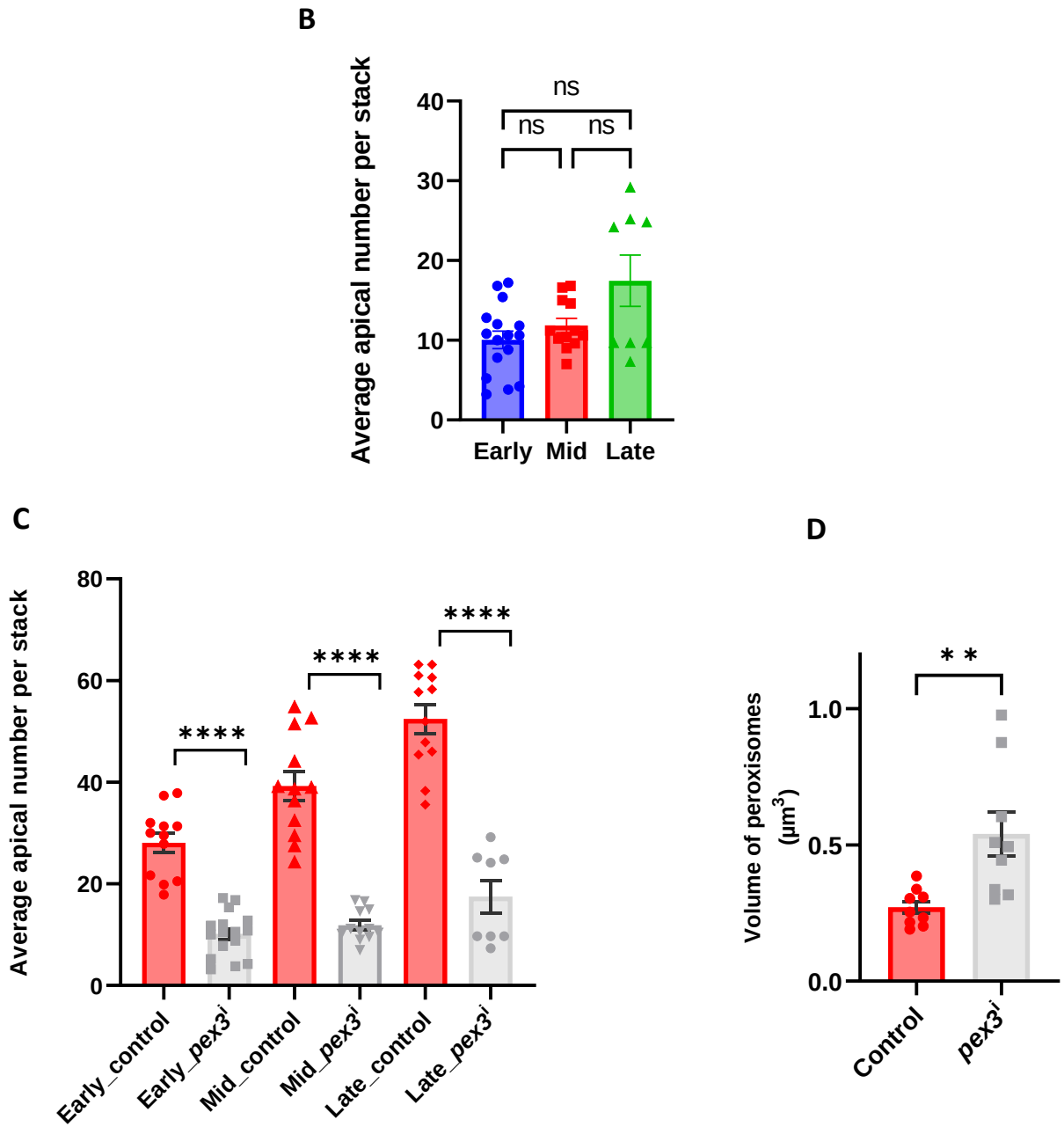

Figure-13 Enlarged size and lesser number of peroxisomes in *pex3* RNAi expressing embryos. Mitochondria is marked with Streptavidin (Green), Peroxisome is stained with anti-SKL tag (Red), membrane is marked with phalloidin (Gray), and composite section showing Phalloidin and anti-SKL together. Scale bar is 10µm **(A).** No change in the number of Peroxisomes in *pex3*^{i} embryos in the apical region per section from early (blue, B) to mid (red, B) and late (green, B) cellularization. **(B).** Reduced number of average apical number of peroxisomes per stack in Pex3i expressing embryos as compared to control across each stage of cellularization **(C)**. Larger size (or

volume) of Peroxisomes in *pex3*^{i} embryos as compared to control **(D)**. This was quantified from n = 3 embryos for each stage, with four sections of 34.2 * 34.2 µm from each embryo. The data is represented as mean ± SEM, with significance levels denoted as follows: * for $p < 0.05$, ** for $p < 0.01$, *** for $p < 0.001$, and **** for $p < 0.0001$. These values were determined using a two-tailed Mann-Whitney test.

3.2.3 Downregulation of PEX5, PEX1, PEX11, PEX14, PEX23 and PEX12 proteins does not affect peroxisome number during *Drosophila* cellularization

In our investigation of the roles played by various PEX proteins, including PEX 5, PEX 1, PEX11, PEX14, PEX23, and PEX12, in peroxisome biogenesis and morphology regulation, we employed RNA interference (RNAi) to inhibit the PEX proteins expression in embryos using nanos-Gal4, then analyzed the embryos with fixed imaging techniques. However, the results revealed no significant alterations in peroxisome numbers or morphology compared to the control **(Figure 14)**.

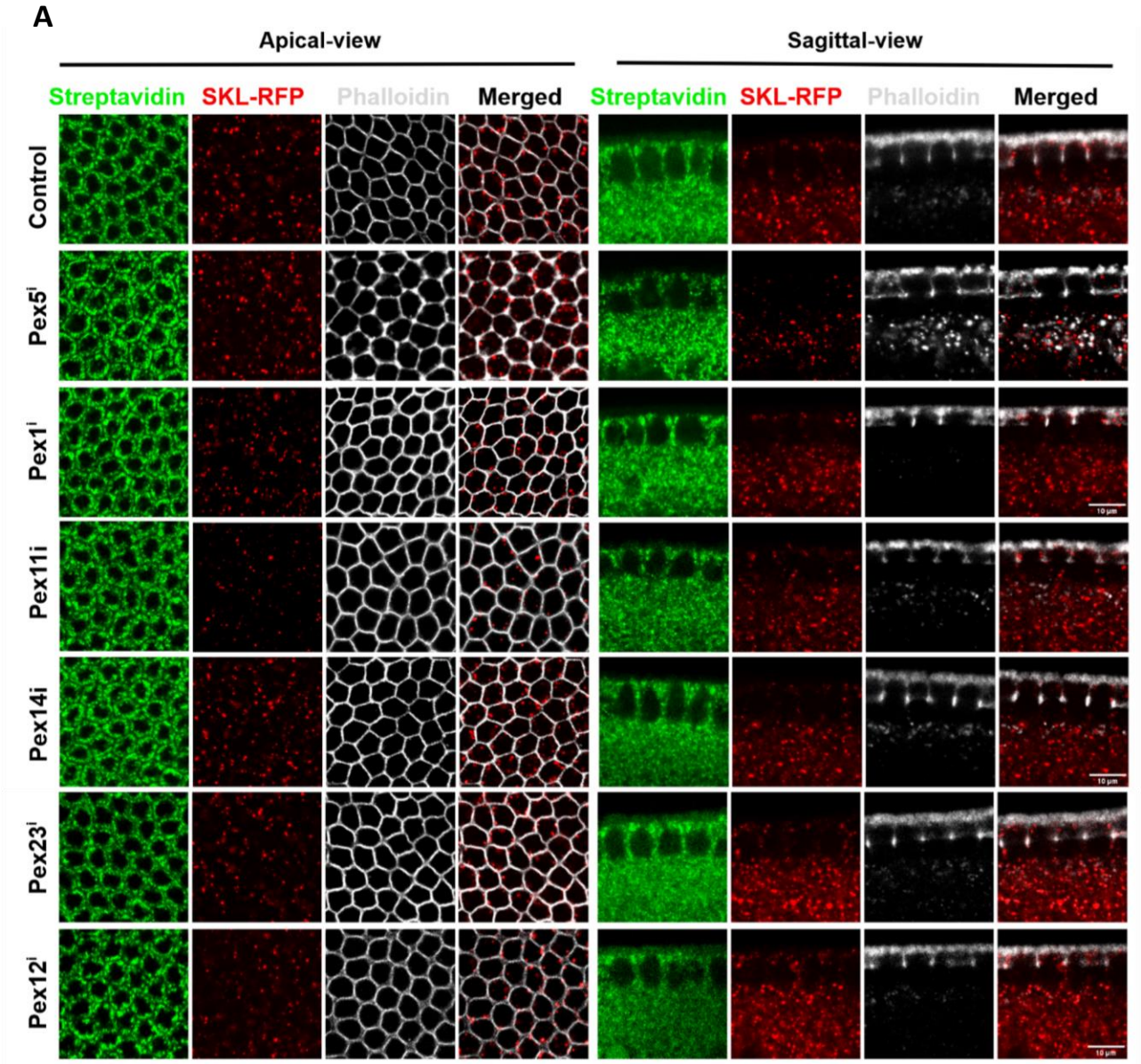
A
Apical-view
Sagittal-view
Streptavidin
SKL-RFP
Phalloidin
Merged
Streptavidin
SKL-RFP
Phalloidin
Merged
Control
Pex5i
Pex1i
Pex11i
Pex14i
Pex23i
Pex12i

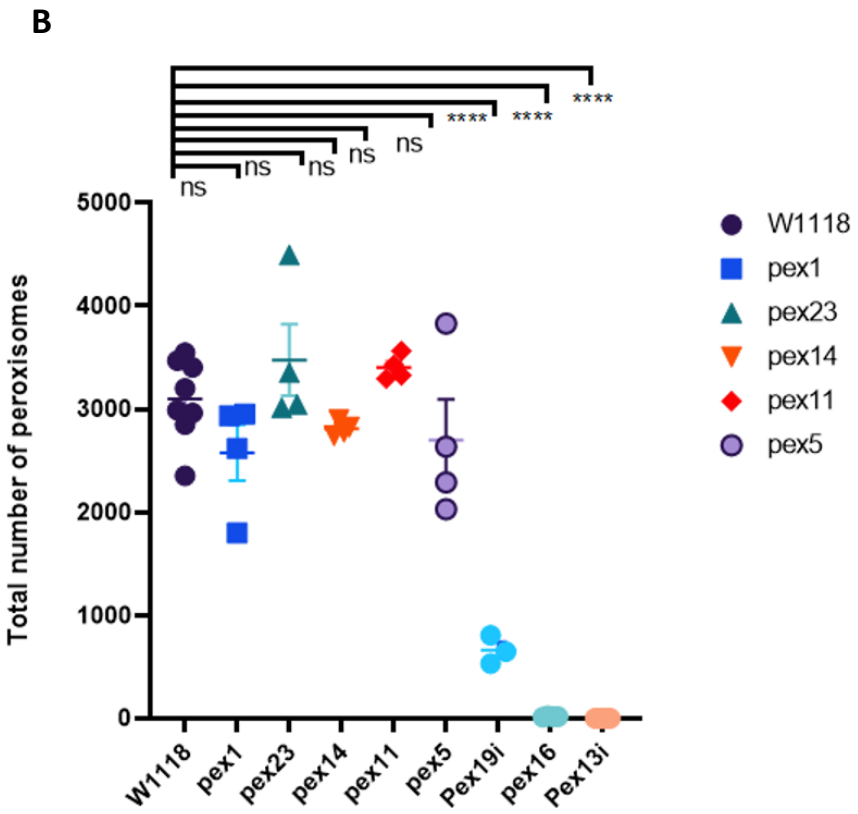

Figure-14. No change in the Peroxisome Number during *Drosophila* cellularization in the *pex5*^{i}, *pex1*^{i}, *pex11*^{i}, *pex14*^{i}, *pex23*^{i} and *pex12*^{i} embryos. Mitochondria is marked with Streptavidin (Green), Peroxisome is marked with GAL4 driven UASp-SKL-RFP tag (Red), membrane is marked with phalloidin (Gray), and composite section showing Phalloidin and SKL-RFP together. Scale bar is 10µm **(A)**. Quantitative analysis of the total peroxisome's count in the PEX mutants (*pex1*^{i}, *pex 3*^{i}, *pex5*^{i}, *pex11*^{i}, *pex13*^{i}, *pex16*^{i}, *pex19*^{i}, *and pex23*^{i}) **(B)**. The data is represented as mean ± SEM, with significance levels denoted as follows: * for $p < 0.05$, ** for $p < 0.01$, *** for $p < 0.001$, and **** for $p < 0.0001$. These values were determined using a two-tailed Mann-Whitney test.

3.3 - Depletion of the Drp1(mitochondrial fission protein) results in fused peroxisomes and a decrease in their quantity.

Drp1 has been demonstrated to play a role in the fission processes of both mitochondria and peroxisomes across different systems. To investigate whether Drp1 is required for peroxisomal fission during these processes, we employed a maternal depletion approach by overexpressing a mutant form of the Drp1 GTPase domain, referred to as Drp1^{SG}, under the control of the nanos-Gal4 promoter. Prior research within our laboratory has previously demonstrated that Drp1^{SG} embryos exhibited a distinct

mitochondrial phenotype, characterized by clustered mitochondria, during the cellularization stage (Chowdhary et al., 2020). Building upon this foundation, our current findings indicate a noticeable alteration in peroxisomal morphology. Specifically, peroxisomes in Drp1^{SG} embryos appear to be enlarged, predominantly showing a fused state **(Figure 15)**. We also did a quantitative assessment of peroxisome abundance in the apical region of the cell in Drp1^{SG} mutant embryos and comparing it to a control group. Our analysis revealed a significant reduction in peroxisome's abundance at the apical region of Drp1^{SG} mutant embryos when compared to the control group.

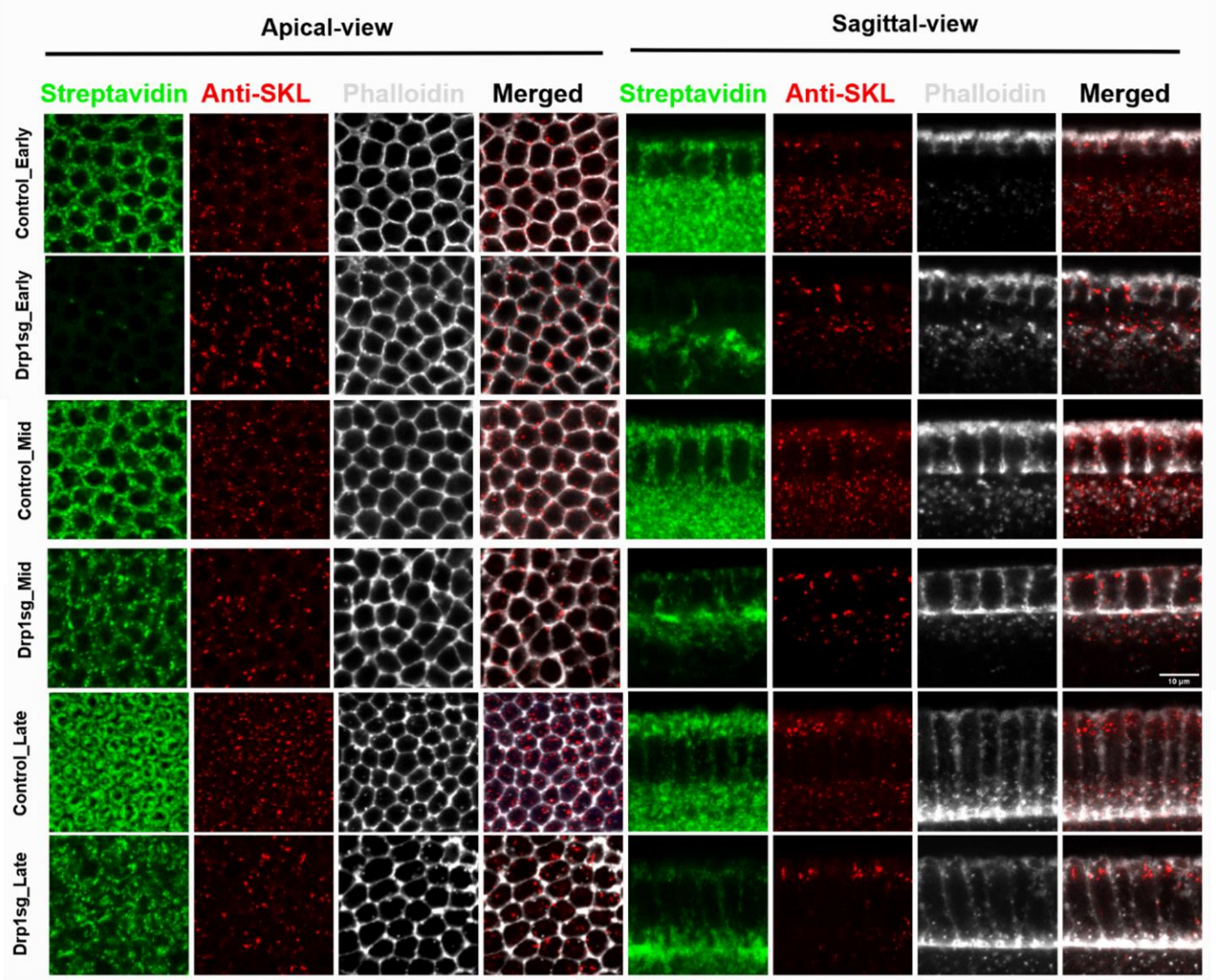

B

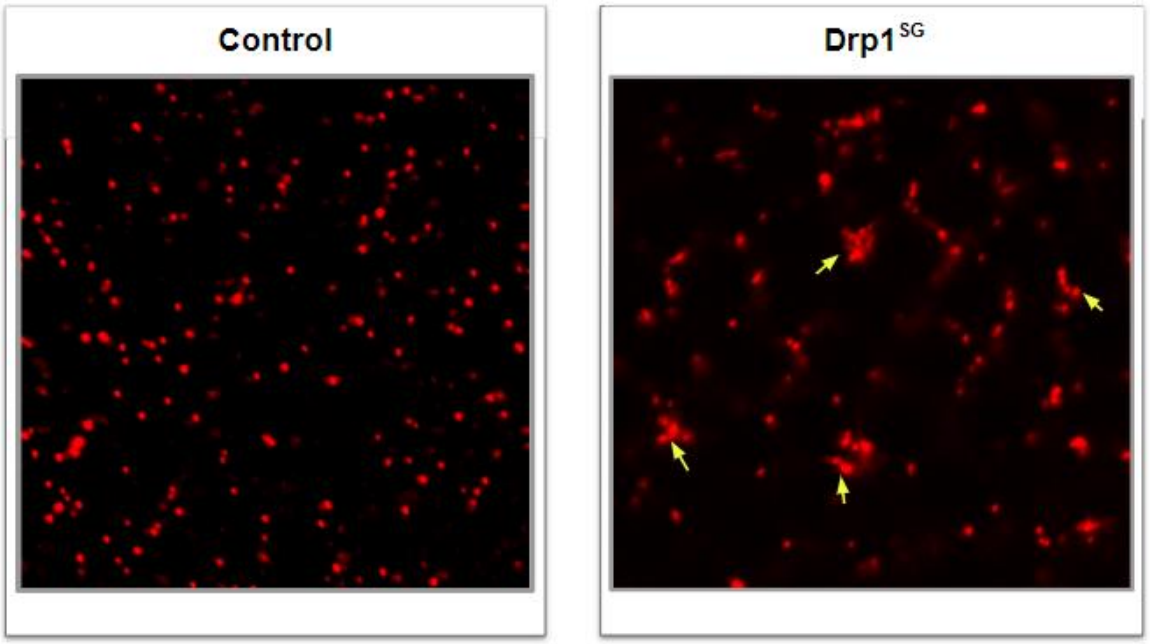

C

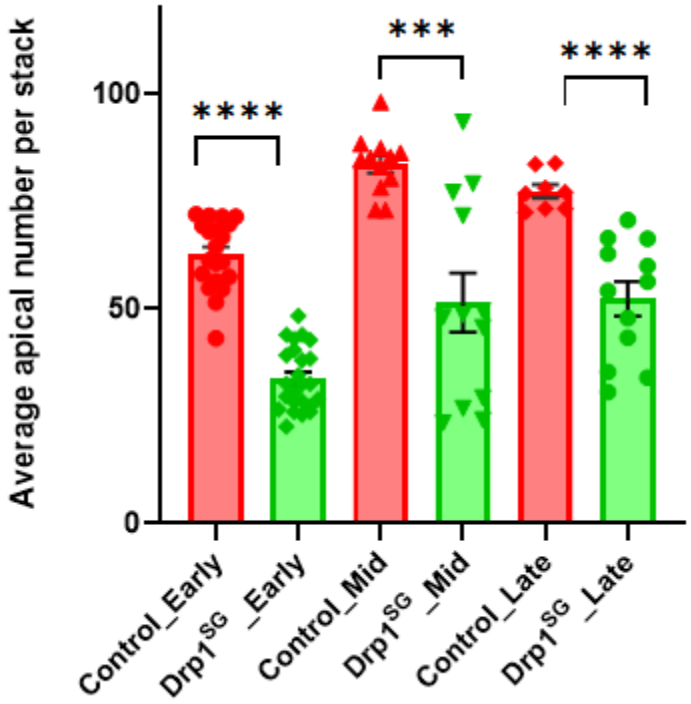

Figure-15 Enlarged (or fused) peroxisomal morphology in Drp1^{SG}. Mitochondria is marked with Streptavidin (Green), Peroxisome is marked with GAL4 driven UASp-SKL-RFP tag (Red), membrane is marked with phalloidin (Gray), and composite section showing Phalloidin and SKL-

RFP together **(A).** Zoomed in view of xy image of SKL-RFP in control and $Drp1^{SG}$ showing the enlarged and clustered peroxisomes in $Drp1^{SG}$ embryos **(B).** Quantitative analysis of peroxisome numbers per stack at the apical region indicated a lower count in $Drp1^{SG}$ embryos across early, mid, and late stages of cellularization when compared to the control group. **(C).** This was quantified from n = 3 embryos for each stage, with four sections of 34.2 * 34.2 µm from each embryo. The data is represented as mean ± SEM, with significance levels denoted as follows: * for $p < 0.05$, ** for $p < 0.01$, *** for $p < 0.001$, and **** for $p < 0.0001$. These values were determined using a two-tailed Mann-Whitney test.

3.4 Increase in Peroxisomes Numbers upon SOD2 depletion in *Drosophila* cellularization.

Peroxisomes and mitochondria house several reactive oxygen species (ROS) scavengers, including enzymes like catalase and superoxide dismutase (SOD), which play a crucial role in reducing ROS levels, thereby preventing oxidative stress. We employed RNA interference (RNAi) to inhibit SOD2 expression in embryos using nanos-Gal4, then analyzed the embryos with fixed imaging techniques. Hence, to investigate the impact of SOD mutants on the quantities and dynamics of peroxisomes during the cellularization stage of *Drosophila* embryogenesis. We expressed RNAi to knock down mitochondrially targeted SOD2 with nanos-Gal4 and stained the embryos via fixed imaging (Figure 16 A) and live imaging (Figure 16 C and E) techniques. The results of our study demonstrate a significant increase in peroxisome numbers in the $sod2^{i}$ mutants (Figure 16 B). This notable increase may be linked to the cellular response to elevated ROS levels within the cells, a phenomenon previously observed in $sod2^{i}$ mutants.

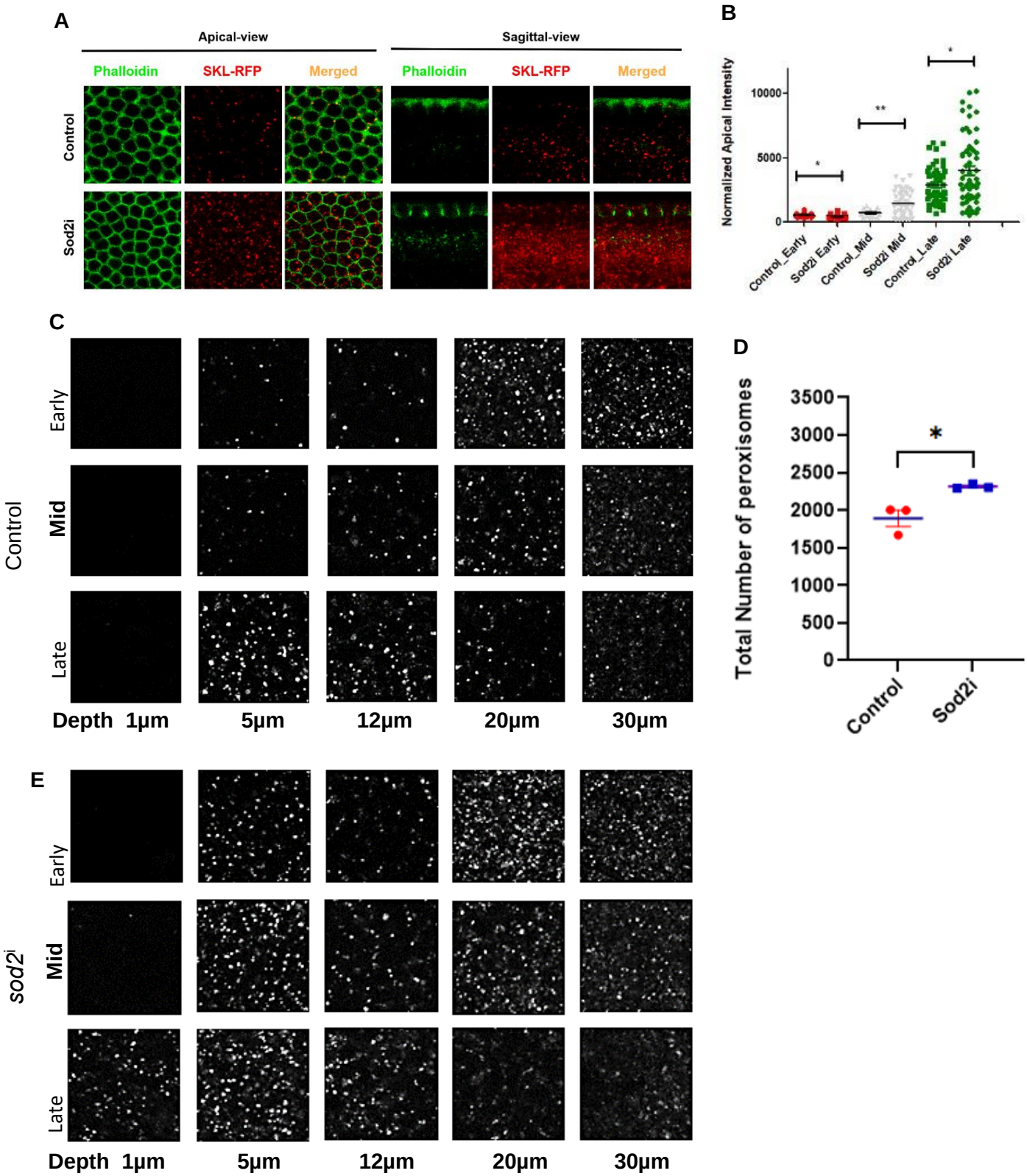

Figure-16 Elevated number of peroxisomes in *sod2*^{i} mutant. (A) The peroxisome is marked with GAL4 driven UASp-SKL-RFP tag (Red), the membrane is marked with phalloidin (Green), and the

composite section shows Phalloidin and SKL-RFP together. **(B)** the graph represents the quantitative analysis of normalized apical intensity for peroxisomes in control and *sod2*^{i} expressing embryos. Images captured from the live imaging of these embryos is represented at various depths, ranging from 1µm to 30µm for different stages of cellularization in control **(C)** and *sod2*^{i} embryos **(E)** expressing SKL-RFP show an increase in SKL- RFP signal in *sod2*^{i} mutant as compared to control. Quantitative analysis of total peroxisome's count **(D)** in the *sod2*^{i} and control also showed the same results. The data is represented as mean ± SEM, with significance levels denoted as follows: * for $p < 0.05$, ** for $p < 0.01$, *** for $p < 0.001$, and **** for $p < 0.0001$. These values were determined using a two-tailed Mann-Whitney test.

3.5 Elevated levels of reactive oxygen species (ROS) mitigate defects in peroxisome numbers observed in Drp1 mutant embryos.

In Drp1^{SG} mutant embryos, mitochondrial clustering during cellularization has been observed (Chowdhary et al., 2020). Given Drp1's involvement in peroxisomal fission, enlarged or fused peroxisomes were observed during cellularization, along with a reduced peroxisome count compared to control embryos. Drp1^{SG} embryos exhibited lower ROS levels than controls (as published earlier). To investigate ROS's role in regulating peroxisome numbers, peroxisome counts were assessed in mutants with elevated ROS levels, such as *sod2*^{i} mutants. Interestingly, an increase in peroxisome's count was observed in *sod2*^{i} mutants, suggesting ROS elevation may enhance peroxisome proliferation.

Subsequently, peroxisome numbers were examined in Drp1^{SG}; *sod2*^{i} embryos, hypothesizing an increase compared to Drp1^{SG} embryos. Remarkably, our experimental results (as shown in **Figure 17A**) validated the hypothesis, confirming an increase in peroxisome numbers in Drp1^{SG}; *sod2*^{i} embryos compared to Drp1^{SG} mutants. Notably, the quantitative analysis **(Figure 17B)** also shows that Drp1^{SG}; *sod2*^{i} embryos exhibited significantly higher apical peroxisome counts than Drp1^{SG} mutants, particularly during early and late cellularization stages. This suggests that increasing ROS levels suppress peroxisome number defects.

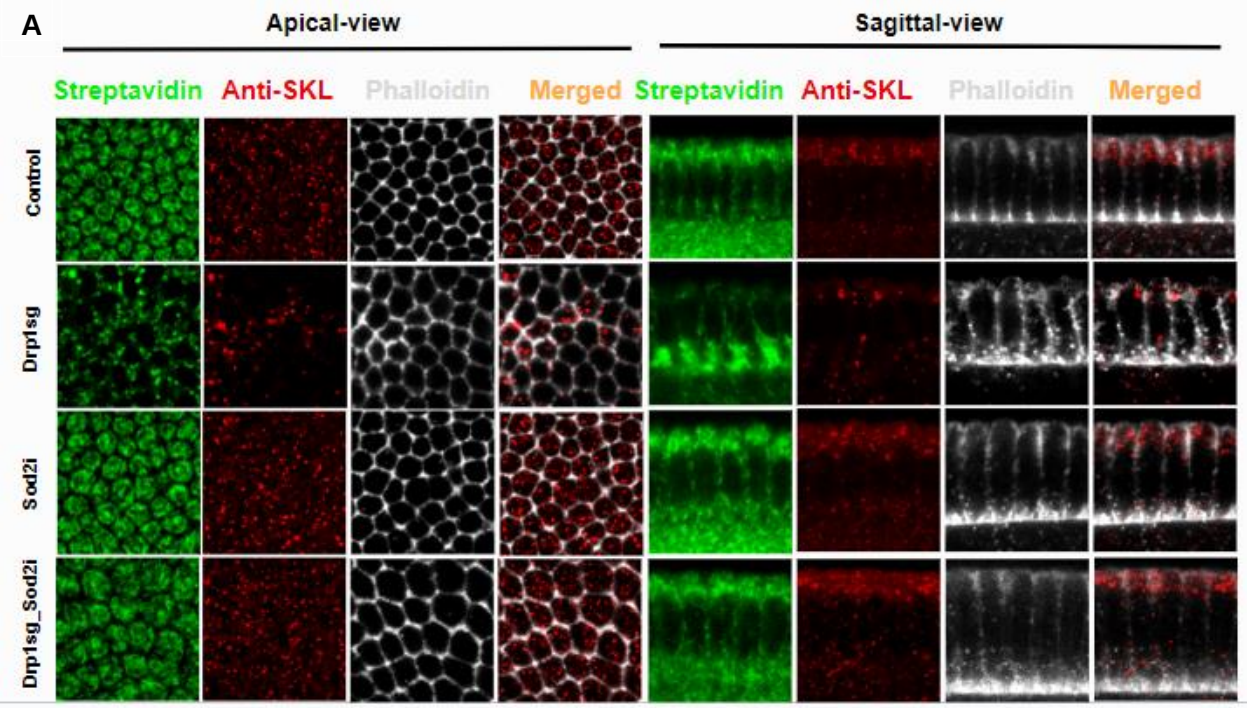
A
Apical-view
Sagittal-view
Streptavidin
Anti-SKL
Phalloidin
Merged
Streptavidin
Anti-SKL
Phalloidin
Merged
Control
Drp1sg
Sod2i
Drp1sg_Sod2i

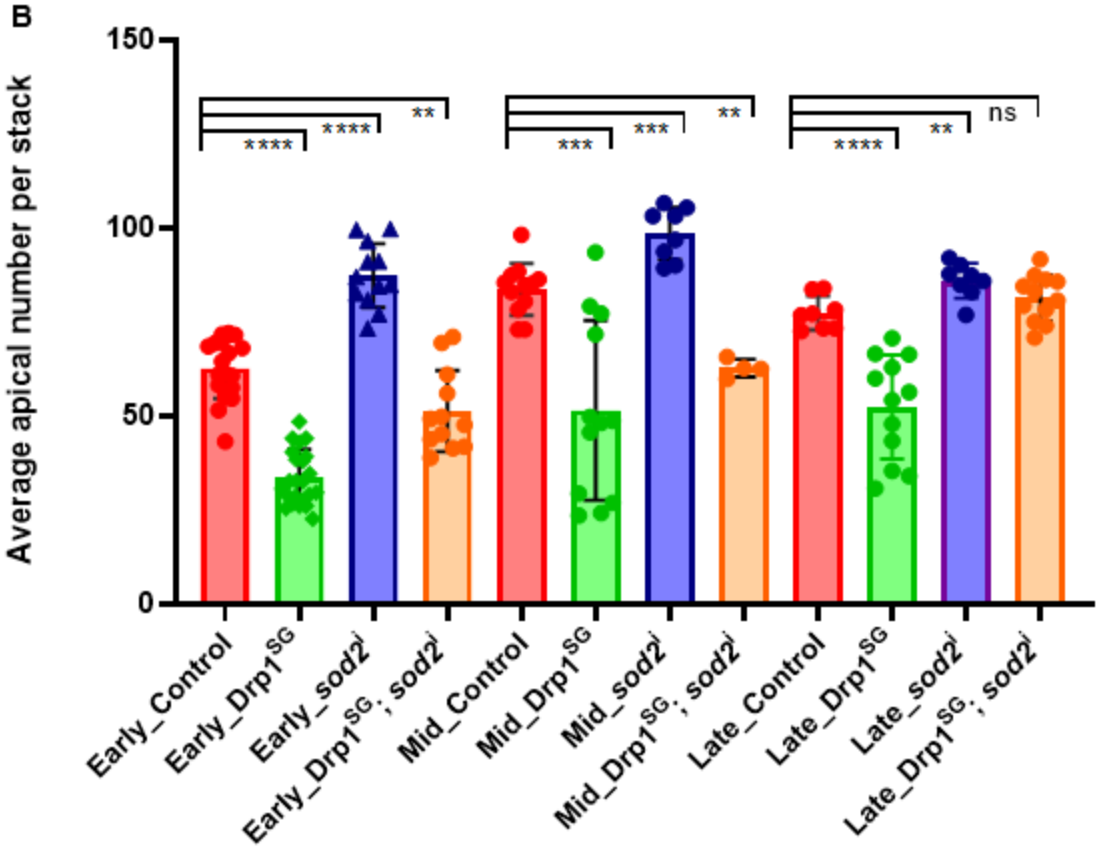
B
Average apical number per stack
150
100
50
0
****
****
**
***
***
**
****
**
ns
Early_Control
Early_Drp1SG
Early_sod2i
Early_Drp1SG; sod2i
Mid_Control
Mid_Drp1SG
Mid_sod2i
Mid_Drp1SG; sod2i
Late_Control
Late_Drp1SG
Late_sod2i
Late_Drp1SG; sod2i

Figure-17 Peroxisome's number defects in Drp1^{SG} is suppressed in Drp1^{SG}; *sod2*^{i} embryos. **(A)** The peroxisome is marked anti-SKL tag (Red), mitochondria is stained with streptavidin (green), the membrane is marked with phalloidin (Green), and the composite section showing the membrane and peroxisomes together apically and sagittally in late cellularizing embryo. **(B)** The graph represents the quantitative analysis of normalized average apical number of peroxisomes in control (red), Drp1^{SG} (green), *sod2*^{i} (blue), and Drp1^{SG}; *sod2*^{i} (orange) embryos. The apical number of peroxisomes in Drp1^{SG}; *sod2*^{i} (orange) is significantly higher than the Drp1^{SG} mutant (green) in early and late stages of cellularization, indicating suppression of numbers defect. n = 3, 3, 3, 3 embryos with four sections of 34.2 * 34.2 µm from each embryo for early, mid, and late stages, respectively are quantified for each genotype. Data is represented as mean ± SEM, * $p < 0.05$, ** $p < 0.01$, ***$p < 0.001$, ****, $p < 0.0001$, Two-tailed, Mann-Whitney test.

Chapter 4 Discussion

Peroxisomes, versatile organelles that are integral to various metabolic pathways such as fatty acid beta-oxidation and amino acid catabolism, play a central role in cellular homeostasis. The results of our study shed light on the distribution and dynamic behaviour of peroxisomes during *Drosophila* embryogenesis and the key proteins influencing their biogenesis and distribution. As our results showed that peroxisomes tend to accumulate in the apical region as cellularization progresses in *Drosophila*. This dynamic shift in peroxisomal distribution suggests that their spatial arrangement maybe intricately linked to developmental processes. Knockdown experiments targeting PEX13 and PEX16 proteins resulted in the complete absence of peroxisomes, while knockdown of PEX19 and PEX3 led to a reduction in the number of peroxisomes during *Drosophila* cellularization. This highlights the role played by these specific PEX proteins in peroxisome biogenesis. Notably, the downregulation of PEX5, PEX1, PEX11, PEX14, PEX23, and PEX12 proteins did not seem to affect peroxisomes morphology or numbers during *Drosophila* cellularization. This implies that their functions may be more relevant at different stages of peroxisomal dynamics or that there might be redundancy in their roles. The $Drp1^{SG}$ mutant embryos exhibited larger, fused peroxisomes, emphasizing Drp1's role in peroxisomal fission. Significant increase in peroxisome numbers in the mitochondrially targeted *sod2* RNAi mutants can be associated with the elevated ROS levels in these mutants. This demonstrates the adaptability of peroxisomes in response to heightened oxidative stress, aligning with their role in ROS scavenging. Furthermore, the suppression of peroxisome number defects in $Drp1^{SG}$; $sod2^{i}$ mutants highlights the highly dynamic nature of peroxisome biogenesis, which is likely influenced by cellular ROS levels.

In summary, our findings offer valuable insights into the dynamic nature of peroxisomes during *Drosophila* embryogenesis, showing that their localization and abundance are associated with various protein factors. While certain PEX proteins, such as PEX13, PEX16, PEX3 and PEX19, are central for peroxisome biogenesis and distribution, others seem to have more specialized or redundant functions. The $Drp1^{SG}$ mutant

results highlight the importance of Drp1 protein in peroxisomal fission, while the adaptability of peroxisomes in *sod2*^{i} mutants and suppression of the defects in the peroxisomes number in Drp1^{SG}; *sod2*^{i} embryos highlights their role in responding to oxidative stress. Overall, our findings contribute to a deeper understanding of peroxisome biology and its regulation during critical developmental processes in *Drosophila*. And, we aim to uncover their potential interactions with the diverse cellular processes during embryogenesis.

Below is a summary model diagram describing the same.

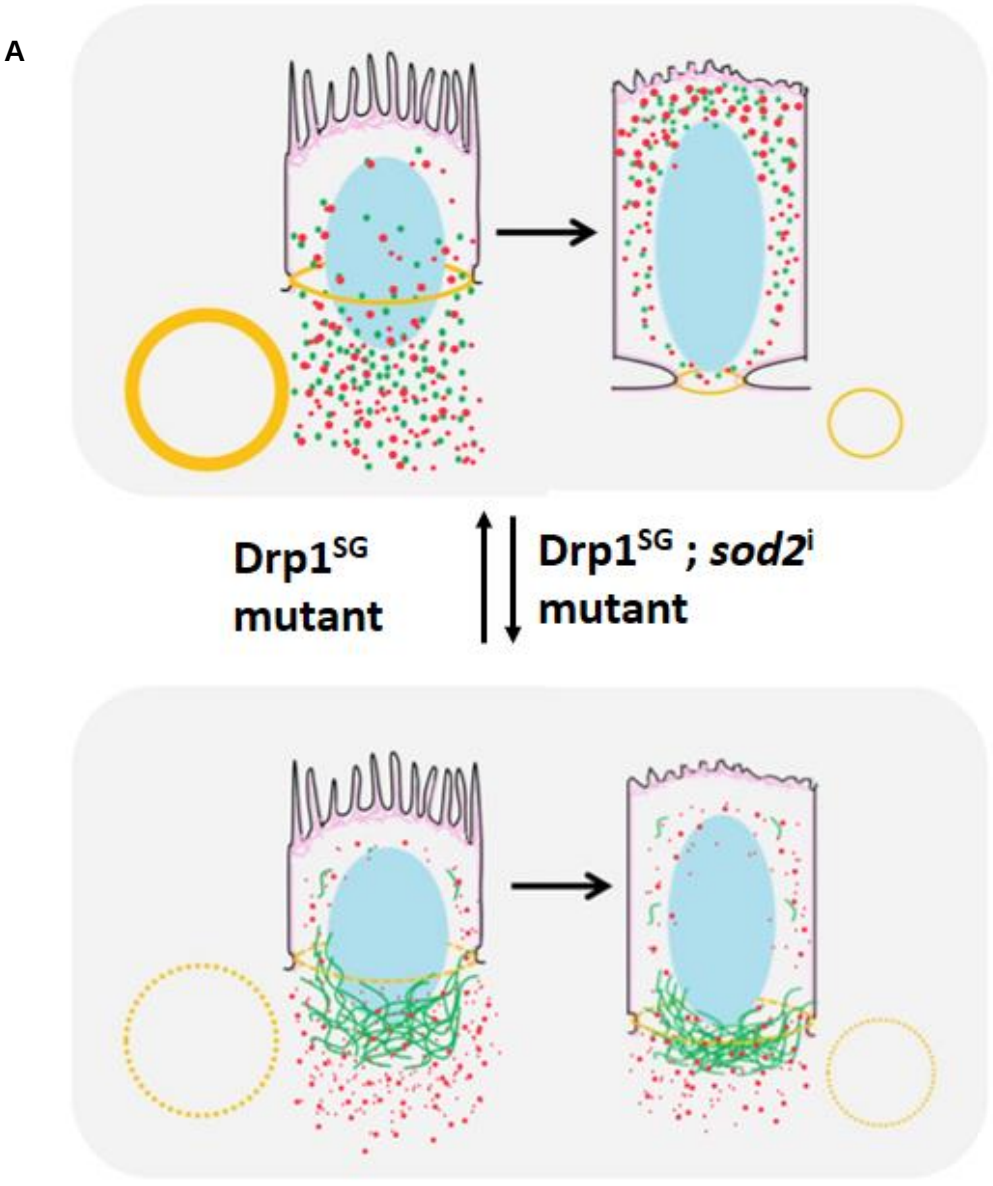

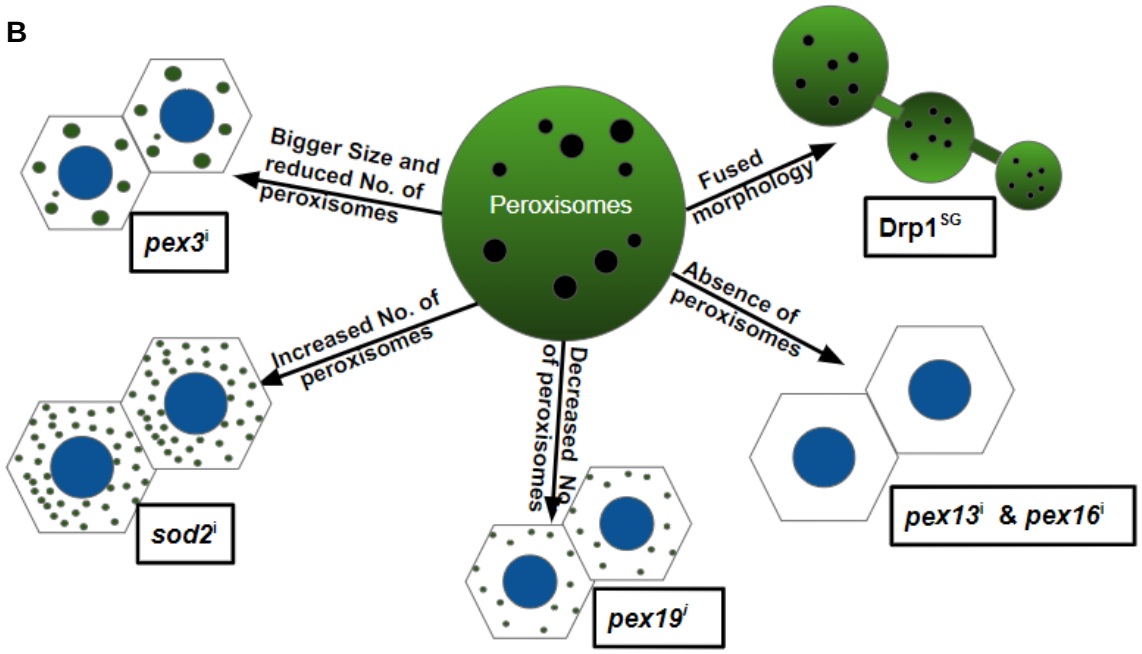

Figure-18 Schematic showing the summary model diagram. (A) model depicting the apical accumulation of peroxisomes as cellularization progresses in *Drosophila*. The fused morphology of peroxisomes and their decreased numbers observed in Drp1^{SG} mutants, along with the suppression of peroxisome number defects in Drp1^{SG}; *sod2*^{i} embryos, highlights the highly dynamic nature of peroxisome biogenesis, which is likely influenced by cellular ROS levels (adapted from Sayali's thesis). **(B)** illustration showing the alterations in peroxisome shape, size and numbers resulting from the knockdown of key regulatory factors such as PEX proteins and Drp1 (fission protein) involved in peroxisome biogenesis pathways.

References

1. Caulfleld, J B, and B F Trump. “Correlation of ultrastructure with function in the rat kidney.” The American journal of pathology vol. 40,2 (1962): 199-218.
2. De Duve, C, and P Baudhuin. “Peroxisomes (microbodies and related particles).” Physiological reviews vol. 46,2 (1966): 323-57.
3. Yamamoto, K, and H D Fahimi. “Three-dimensional reconstruction of a peroxisomal reticulum in regenerating rat liver: evidence of interconnections between heterogeneous segments.” The Journal of cell biology vol. 105,2 (1987): 713-22.
4. Walker, Cheryl L et al. “Redox Regulation of Homeostasis and Proteostasis in Peroxisomes.” Physiological reviews vol. 98,1 (2018): 89-115.
5. Bonekamp, Nina A et al. “Reactive oxygen species and peroxisomes: struggling for balance.” BioFactors (Oxford, England) vol. 35,4 (2009): 346-55. doi:10.1002/biof.48
6. Fransen, Job et al. “Differences in physical fitness and gross motor coordination in boys aged 6-12 years specializing in one versus sampling more than one sport.” Journal of sports sciences vol. 30,4 (2012): 379-86. doi:10.1080/02640414.2011.642808
7. Poirier, Paul et al. “Obesity and cardiovascular disease: pathophysiology, evaluation, and effect of weight loss.” Arteriosclerosis, thrombosis, and vascular biology vol. 26,5 (2006): 968-76. doi:10.1161/01.ATV.0000216787.85457.f3
8. Fujiki, Yukio et al. “Recent insights into peroxisome biogenesis and associated diseases.” Journal of cell science vol. 133,9 jcs236943. 11 May. 2020, doi:10.1242/jcs.236943
9. Hayashi, M et al. “Functional transformation of plant peroxisomes.” Cell biochemistry and biophysics vol. 32 Spring (2000): 295-304. doi:10.1385/cbb:32:1-3:295
10. Lodhi, Irfan J, and Clay F Semenkovich. “Peroxisomes: a nexus for lipid metabolism and cellular signaling.” Cell metabolism vol. 19,3 (2014): 380-92. doi:10.1016/j.cmet.2014.01.002
11. Knoblach, Barbara, and Richard A Rachubinski. “Reconstitution of human peroxisomal β-oxidation in yeast.” FEMS yeast research vol. 18,8 (2018): foy092. doi:10.1093/femsyr/foy092
12. Steinberg, Steven J et al. “Peroxisome biogenesis disorders.” Biochimica et biophysica acta vol. 1763,12 (2006): 1733-48. doi:10.1016/j.bbamcr.2006.09.010
13. Deori, Nayan M et al. “Peroxisomes: role in cellular ageing and age related disorders.” Biogerontology vol. 19,5 (2018): 303-324. doi:10.1007/s10522-018-9761-9

14. Koch, Annett et al. “Dynamin-like protein 1 is involved in peroxisomal fission.” The Journal of biological chemistry vol. 278,10 (2003): 8597-605. doi:10.1074/jbc.M211761200
15. Motley, Alison M, and Ewald H Hettema. “Yeast peroxisomes multiply by growth and division.” The Journal of cell biology vol. 178,3 (2007): 399-410. doi:10.1083/jcb.200702167
16. Opaliński, Łukasz et al. “Membrane curvature during peroxisome fission requires Pex11.” The EMBO journal vol. 30,1 (2011): 5-16. doi:10.1038/emboj.2010.299
17. Nagotu S, et al. (2008) Peroxisome fission in Hansenula polymorpha requires Mdv1 and Fis1, two proteins also involved in mitochondrial fission. Traffic 9(9):1471-84
18. Raychaudhuri, Sumana, and William A Prinz. “Nonvesicular phospholipid transfer between peroxisomes and the endoplasmic reticulum.” Proceedings of the National Academy of Sciences of the United States of America vol. 105,41 (2008): 15785-90. doi:10.1073/pnas.0808321105
19. Hoepfner, Dominic et al. “Contribution of the endoplasmic reticulum to peroxisome formation.” Cell vol. 122,1 (2005): 85-95. doi:10.1016/j.cell.2005.04.025
20. Dimitrov, Lazar et al. “The role of the endoplasmic reticulum in peroxisome biogenesis.” Cold Spring Harbor perspectives in biology vol. 5,5 a013243. 1 May. 2013, doi:10.1101/cshperspect.a013243
21. Agrawal, Gaurav, and Suresh Subramani. “De novo peroxisome biogenesis: Evolving concepts and conundrums.” Biochimica et biophysica acta vol. 1863,5 (2016): 892-901. doi:10.1016/j.bbamcr.2015.09.014
22. Sugiura, Ayumu et al. “Newly born peroxisomes are a hybrid of mitochondrial and ER-derived pre-peroxisomes.” Nature vol. 542,7640 (2017): 251-254. doi:10.1038/nature21375
23. Sesaki H, Adachi Y, Kageyama Y, Itoh K, Iijima M (2014) In vivo functions of Drp1: lessons learned from yeast genetics and mouse knockouts. Biochim Biophys Acta 1842: 1179–1185
24. Kobayashi S, Tanaka A, Fujiki Y (2007) Fis1, DLP1, and Pex11p coordinately regulate peroxisome morphogenesis. Exp Cell Res 313: 1675–1686
25. Yoshida Y, Niwa H, Honsho M, Itoyama A, Fujiki Y (2015) Pex11mediates peroxisomal proliferation by promoting deformation of the lipid membrane. Biol Open 4: 710–721
26. Fan, Jinjiang et al. “ACBD2/ECI2-Mediated Peroxisome-Mitochondria Interactions in Leydig Cell Steroid Biosynthesis.” Molecular endocrinology (Baltimore, Md.) vol. 30,7 (2016): 763-82. doi:10.1210/me.2016-1008
27. Mattiazzi Ušaj M, Brložnik M, Kaferle P, Žitnik M, Wolinski H, Leitner F, Kohlwein SD, Zupan B, Petrovič U (2015) Genome-wide localization study of yeast Pex11

identifies peroxisome-mitochondria interactions through the ERMES complex. J Mol Biol 427: 2072–2087

28. Fransen, Marc, and Celien Lismont. “Peroxisomes and Cellular Oxidant/Antioxidant Balance: Protein Redox Modifications and Impact on Inter-organelle Communication.” Sub-cellular biochemistry vol. 89 (2018): 435-461. doi:10.1007/978-981-13-2233-4_19

29. Costello, Joseph L et al. “ACBD5 and VAPB mediate membrane associations between peroxisomes and the ER.” The Journal of cell biology vol. 216,2 (2017): 331-342. doi:10.1083/jcb.201607055

30. Torres, S. E., Gallagher, C. M., Plate, L., Gupta, M., Liem, C. R., Guo, X., et al. (2019). Ceapins block the unfolded protein response sensor ATF6alpha by inducing a neomorphic inter-organelle tether. eLife 8:e46595.

31. Schrader, M., Grille, S., Fahimi, H. D., and Islinger, M. (2013). Peroxisome interactions and cross-talk with other subcellular compartments in animal cells. Subcell. Biochem. 69, 1–22. doi: 10.1007/978-94-007-6889-5_1

32. Kong, J., Ji, Y., Jeon, Y. G., Han, J. S., Han, K. H., Lee, J. H., et al. (2020). Spatiotemporal contact between peroxisomes and lipid droplets regulates fasting-induced lipolysis via PEX5. Nat. Commun. 11:578.

33. Chang, C. L., Weigel, A. V., Ioannou, M. S., Pasolli, H. A., Xu, C. S., and Peale, D. R. (2019). Spastin tethers lipid droplets to peroxisomes and directs fatty acid trafficking through ESCRT-III. J. Cell Biol. 218, 2583–2599. doi: 10.1083/jcb.201902061

34. Chu, B. B., Liao, Y. C., Qi, W., Xie, C., Du, X., Wang, J., et al. (2015). Cholesterol transport through lysosome-peroxisome membrane contacts. Cell 161, 291–306. doi: 10.1016/j.cell.2015.02.019

35. Zhang, J., Kim, J., Alexander, A., Cai, S., Tripathi, D. N., and Dere, R. (2013). A tuberous sclerosis complex signalling node at the peroxisome regulates mTORC1 and autophagy in response to ROS. Nat. Cell Biol. 15, 1186–1196. doi: 10.1038/ncb2822

36. Chen, Chao et al. “Peroxisomal Membrane Contact Sites in Mammalian Cells.” Frontiers in cell and developmental biology vol. 8 512. 23 Jun. 2020, doi:10.3389/fcell.2020.00512

37. DeLuca, Steven Z, and Patrick H O'Farrell. “Barriers to male transmission of mitochondrial DNA in sperm development.” Developmental cell vol. 22,3 (2012): 660-8. doi:10.1016/j.devcel.2011.12.021

38. Sato, Miyuki, and Ken Sato. “Degradation of paternal mitochondria by fertilization-triggered autophagy in C. elegans embryos.” Science (New York, N.Y.) vol. 334,6059 (2011): 1141-4. doi:10.1126/science.1210333

39. Chen, Chien-Tsun et al. “Mitochondrial bioenergetic function and metabolic plasticity in stem cell differentiation and cellular reprogramming.” Biochimica et biophysica acta vol. 1820,5 (2012): 571-6. doi:10.1016/j.bbagen.2011.09.013
40. Dumollard, Rémi et al. “The role of mitochondrial function in the oocyte and embryo.” Current topics in developmental biology vol. 77 (2007): 21-49. doi:10.1016/S0070-2153(06)77002-8
41. Frescas, David et al. “The secretory membrane system in the *Drosophila* syncytial blastoderm embryo exists as functionally compartmentalized units around individual nuclei.” The Journal of cell biology vol. 173,2 (2006): 219-30. doi:10.1083/jcb.200601156
42. Freeman, M et al. “The dissociation of nuclear and centrosomal division in gnu, a mutation causing giant nuclei in *Drosophila*.” Cell vol. 46,3 (1986): 457-68. doi:10.1016/0092-8674(86)90666-5
43. Rikhy, Richa et al. “Dynamin regulates metaphase furrow formation and plasma membrane compartmentalization in the syncytial *Drosophila* embryo.” Biology open vol. 4,3 301-11. 6 Feb. 2015, doi:10.1242/bio.20149936
44. Chowdhary, Sayali et al. “Mitochondrial morphology and activity regulate furrow ingression and contractile ring dynamics in *Drosophila* cellularization.” Molecular biology of the cell vol. 31,21 (2020): 2331-2347. doi:10.1091/mbc.E20-03-0177
45. Mast, Fred D et al. “A *Drosophila* model for the Zellweger spectrum of peroxisome biogenesis disorders.” Disease models & mechanisms vol. 4,5 (2011): 659-72. doi:10.1242/dmm.007419
46. Sharma, Arpit et al. “Causal roles of mitochondrial dynamics in longevity and healthy aging.” EMBO reports vol. 20,12 (2019): e48395. doi:10.15252/embr.201948395